Such a transduction activity of Vpr is energy independent and does not require a cellular receptor [15]. As one of possibly related mechanisms of transducing activity, Vpr forms a channel in cellular membranes [16,17], and the amino-terminal region of 40 aa of Vpr with α-helix structures is responsible for the ion channel formation [17].

Proteins, such as antennapedia of *Drosophila* (ANTP) [18], VP22 of herpes simplex [19], and Tat of HIV-1 [20], are known to possess protein transduction domains (PTD). PTD enables proteins to cross biological membranes and helps them to enter the cytoplasm. It has been also reported that a variety of proteins, when expressed as chimetric proteins with the peptide, enter target cells. PTD has an arginine-rich region, and it was expected that the C-terminal region of Vpr, which contains an arginine-rich stretch, functioned as PTD. It was, however, concluded that the C-terminal half of Vpr did not show any activities as PTD [15], and the region of Vpr responsible for transducing exogenous protein remained to be clarified.

In the present study, we identified a sequence corresponding to the third α-helix domain (C45D18) as PTD. Interestingly, C45D18 entered cells even without cellular growth, and C45D18-conjugated green fluorescent protein (GFP) was quickly transferred to the nucleus. Transduction of protein conjugated with C45D18 was more efficient than that conjugated with Tat-derived peptide. Based on results that C45D18-conjugated proteins were efficiently transduced into cord blood mononuclear (CBMN) cells as well as resting adherent cells, we propose that C45D18 functions as a novel vehicle that facilitates nuclear trafficking of molecules into target cells.

Materials and methods

Cell culture and chemicals. HT1080 and HeLa cells were cultured in Dulbecco's modified Eagle's medium supplemented with 10% fetal calf serum (FCS) (Sigma, SI). Cord blood was kindly provided by volunteers who gave informed consent. CBMN cells were prepared by centrifugation, according to the manufacturer's protocol (Nycomed Pharma AS, Norway). Briefly, cord blood was diluted with the same amount of phosphate buffered saline (PBS) and applied on the Lymphoprep solution. After centrifugation for 20 min at 800g, cells at the interphase were collected, washed once with PBS, and resuspended in Iscove's modified Dulbecco's medium (IMDM) supplemented with 10% FCS. Jurkat cells and HL-60 cells were cultured in IMDM with 10% FCS. To prepare resting cells, HT1080 cells were cultured for 4 days in FCS-free medium. Cell growth of HL-60 cells was also arrested with 1 μg/ml aphidicolin (APC) (Sigma, SI). As a control, dimethyl sulfoxide (DMSO), used as a solvent of APC, was treated.

Peptide synthesis and detection of incorporated peptide. Various types of peptides derived from Vpr (see Fig. 1A) and Tat (GYGRKKRR QRRRGGC, amino acids described as single letters) were chemically synthesized (Wako, Tokyo). Biotin was added at the amino terminal end of each peptide. After treatment of peptides, cells were washed once with PBS and then fixed with 100% ice-cold methanol. To exclude signals associated with cellular membranes, cells were treated for 10 min with 0.2% Triton X-100 in PBS [21]. Cells were then reacted for 1 h with streptavidin (SA)-conjugated FITC (SA-FITC) and washed several times in PBS with 0.05% Tween 20. To detect the interaction of the peptide and plasmid DNA, different doses of the peptide (1–30 μg) were mixed with 0.2 μg plasmid DNA. A reporter plasmid, pCMV/luciferase, was kindly provided by Dr. Shimada (Nihon Medical School). Luciferase activity was assayed, as described [21].

Expression of recombinant green fluorescent protein and conjugation with peptides. A recombinant protein of green fluorescent protein (GFP) tagged with $(His)_6$ was expressed by a baculovirus system with pFASTBAC and purified with proband region (Invitrogen, Carlsbad, CA). Molecular weights of GFP and β-galactosidase (β-gal) (Wako, MI) were about 35 and 465 kDa, respectively. These proteins were chemically conjugated with Vpr-derived peptides (IBL, Fujioka, Japan). Briefly, about 300 μg protein was suspended in 10 mM phosphate buffer (pH 7.0) and added with 0.1 mM *N*-[e-maleimidocaproyloxiy]succinimide ester (DOJINDO Lab. Kumamoto, Japan). After 30 min at room temperature, each Vpr-derived peptide was added and further incubated for 3 h at room temperature. Conjugated molecules were then dialyzed against PBS overnight.

To test protein transduction, cells were incubated with conjugated proteins overnight and incorporated GFP was detected by an antibody. To demonstrate β-gal activity, X-gal staining was carried out according to the method described [22].

Fluorescent activated cell sorter (FACS) analysis. Incorporation of peptides was analyzed by detecting SA-FITC bound to the peptides. For cell-cycle analysis, cells were treated for 1 h with 10 μM bromodeoxyuridine (BrdU) (Sigma, St. Louis, MO). After fixation in 70% ice-cold ethanol, cells were treated with FITC-conjugated anti-BrdU antibody (Beckton–Dickinson, San Jose, CA) and then stained with 5 μM propidium iodide (Sigma). To study the effect of Vpr on cell-cycle, cells after treatment of peptides were stained with 50 μg/ml propidium iodide and subjected to FACS analysis. For FACS analysis of β-galactosidase activity, a FluoReporter lacZ Flow Cytometry Kit (Molecular Probes, Eugene, OR) was used. Briefly, 5×10^5/100 μl of CBMN cells was mixed with 1 mM fluorescein di-β-D-galactopyranoside for 1 min and was added to 1.8 ml of ice-cold PBS containing 1.5 μM propidium iodide. FACS analysis was carried out by Cellquest (Beckton–Dickinson, San Jose, CA).

Results

Identification of Vpr-derived oligopeptide with transducing activity

The carboxyl-half of Vpr has been shown to transduce plasmid DNA into cultured cells [14]. On the other hand, we previously reported that Vpr induced cell-cycle abnormality at the G2/M phase, but Vpr mutant that lacked C-terminal 18 amino acids was negative for the cell-cycle abnormality [9]. Based on these observations, we tested whether C-terminal 45 aa of Vpr without the extreme C-terminal 18 aa (C45D18, Fig. 1A) had a trafficking activity. A biotin-conjugated 27-mer peptide (52–78 aa) was synthesized, and 10 μg/ml of the peptide was added into the medium of cultured cells. On the next day, an incorporated peptide was detected with SA-FITC. As shown in Fig. 1B, C45D18 was clearly detected in the peptide-treated cells (Fig. 1B, middle

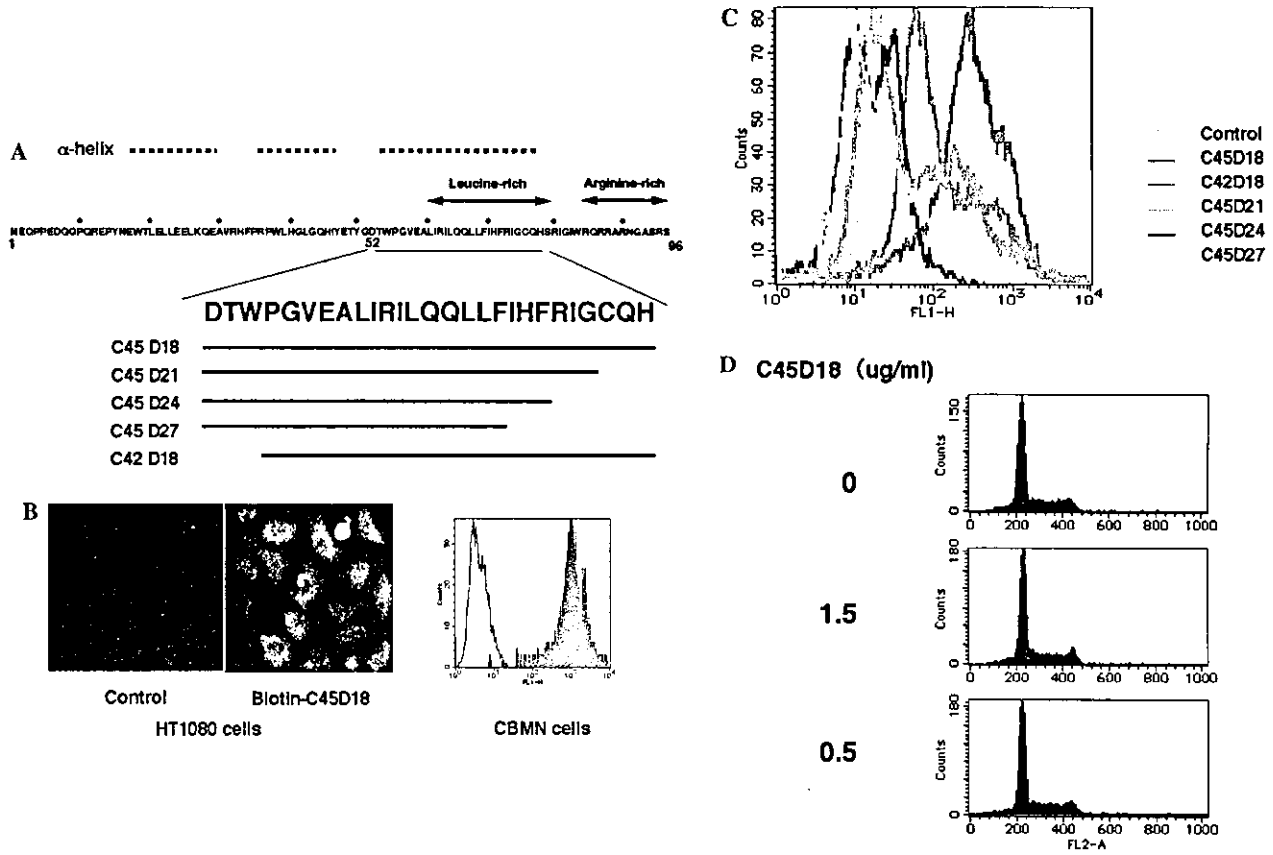

Fig. 1. Identification of Vpr-derived peptide that is incorporated into cells. (A) Amino acid sequence of Vpr used in the present study. (B) Incorporation of C45D18 into cells. Results of HT1080 cells (left panels) and CBMN cells (right panel) are shown. Note that almost all of cells are positive for the incorporated peptide (shown by yellow and red in left and right panels, respectively). (C) Transducing activity of synthetic peptides. Several biotin-conjugated peptides were synthesized and added into the culture medium of CBMN cells. On the next day, the incorporated peptides were detected with SA-FITC. Amino acid sequence of each peptide is shown in (A). (D) Effects of C45D18 on cell-cycle. Cells were treated with C45D18 for 2 days and then subjected to cell-cycle analysis. (For interpretation of the references to colour in this figure legend, the reader is referred to the web version of this paper.)

panel). We observed that C45D18 was also efficiently incorporated into CBMN cells (Fig. 1B, right panel shown by red). FACS analysis revealed that almost 100% of cells were positive for the incorporated peptide after overnight treatment.

To identify the minimal region required for such trafficking activity, several biotinylated peptides were synthesized (Fig. 1A), and we tested whether they were incorporated into CBMN cells, (Fig. 1C). Three peptides of C45D21 (52–75 aa), C45D24 (52–72 aa), and C45D27 (52–69 aa) were less efficiently incorporated to CBMN cells than C45D18 (orange, purple, and yellow peaks, respectively). When amino-terminal three amino acids were deleted from C45D18 (C42D18), its trafficking activity was greatly reduced (blue in Fig. 1C).

It has been reported that Vpr induces cell-cycle abnormality at G2/M phase, and we studied whether C45D18 has an activity on cell-cycle. As shown in Fig. 1D, FACS analysis revealed that cell-cycle was not changed after treatment for 2 days. These data imply that C45D18 is an appropriate sequence for further characterization of the potentiality for transducing activity.

Trafficking macromolecules

We next studied whether C45D18 could transduce plasmid DNA. Consistent with a previous report on the full-length peptide of Vpr [14], C45D18 interacted with plasmid DNA. Unfortunately, however, we could not obtain a favorable amount of exogenous gene expression in cells transfected with the complex (data not shown). To evaluate the activity of C45D18 to transport macromolecules into cells, we studied whether C45D18, when attached to a recombinant protein, entered cells. For this purpose, C45D18 was conjugated at various molar ratios with a purified recombinant protein of GFP and added into the culture medium. On the next day, incorporated proteins were detected. As shown in Fig. 2A, cells treated with C45D18-conjugated GFP were positive for incorporation, although the protein was not detected at all in cells treated with GFP by itself (Fig. 2A, left panel). In the present study, cells were treated with 0.2% Triton X-100 before treatment with SA-FITC. Since this procedure abolished signals associated with cellular membranes [21], our positive ob-

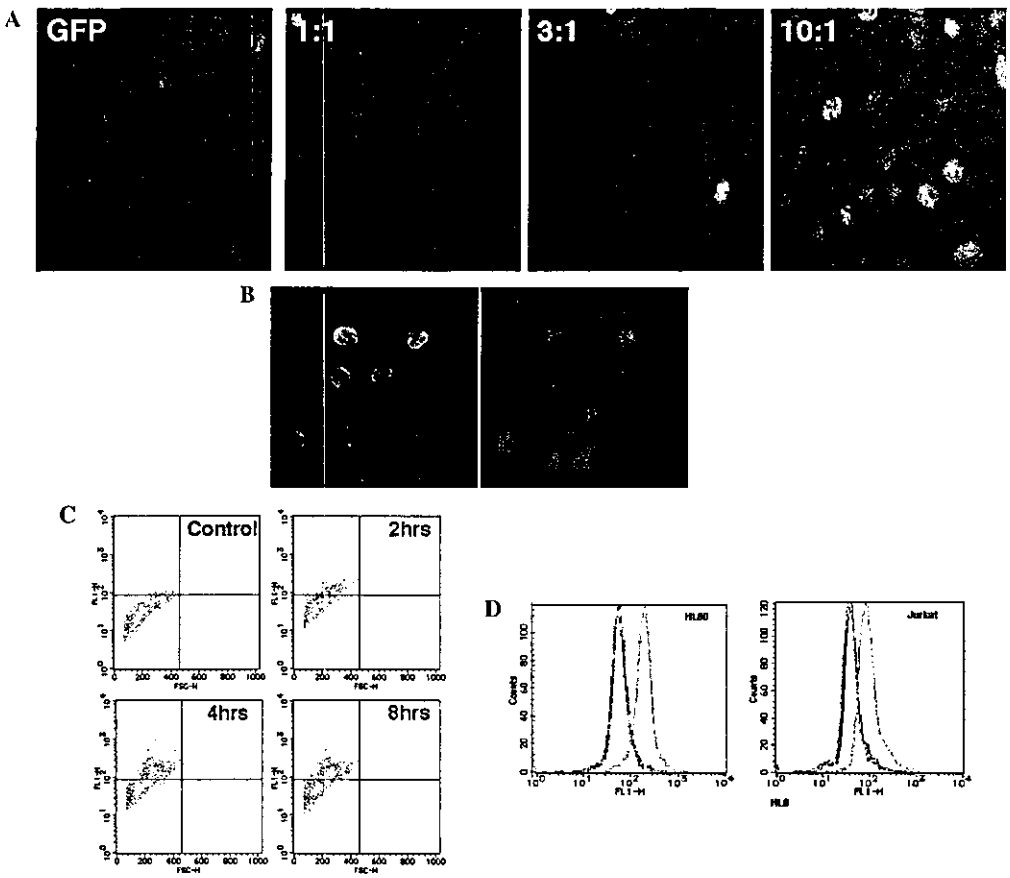

Fig. 2. Trafficking macromolecule by C45D18. (A) Incorporation of C45D18-conjugated GFP into HT1080 cells. GFP conjugated with different doses of C45D18 (3 μg/ml) was added to cells, and the incorporated GFP was detected by immunostaining with an antibody to GFP. The molar ratio of C45D18 to GFP was 1:1, 3:1, and 10:1. As a control just GFP (3 μg/ml) was added into the medium (left panel). (B) Nuclear localization of incorporated C45D18-conjugated GFP. GFP and nuclear DNA were stained with the antibody to GFP and Hoechst 33258. Incorporated GFP was detected by laser-scanning microscopy. Signals of GFP (left panel) and DNA (right panel) on the same field are shown by red and blue, respectively. (C) Time course of the incorporation of CV45D18-conjugated GFP. HL-60 cells were treated with C45D18-conjugated GFP (a molar ration of C45D18: GFP = 10:1) for 2 (upper right panel), 4 (lower left panel), and 8 h (lower right panel). As a control, cells were incubated with the conjugated GFP for 8 h. (D) Efficient trafficking by C45D18 compared to Tat-derived peptide. A chemically synthesized Tat-derived peptide (see Materials and methods) was conjugated to GFP according to the completely same procedures of C45D18, and added into culture medium of HL-60 (left panel) and Jurkat cells (right panel). Incorporated GFP, C45D18-GFP, and Tat-GFP were shown by red, orange, and blue, respectively. Note that C45D18-conjugated GFP was more efficiently incorporated than Tat-GFP. (For interpretation of the references to colour in this figure legend, the reader is referred to the web version of this paper.)

servations indicate that the C45D18-conjugated protein was actually incorporated into cells. The amount of incorporated proteins increased according to doses of C45D18 conjugated to the protein (Fig. 2A). As a further interesting observation, incorporated GFP was detected in the regions corresponding to the nuclei of treated cells. Laser-scanning microscopy clearly detected that the incorporated GFP was present in the nucleus (Fig. 2B, see also Fig. 3C), implying that C45D18 can be used for nuclear trafficking of macromolecules.

Characterization of C45D18-dependent trafficking of macromolecules

We characterized the C45D18-dependent incorporation of GFP. To accurately measure the population with incorporated GFP, HL-60 cells were treated with the C45D18-GFP (molar ratio = 10:1) and subjected to FACS analysis. First, the dose–response of the incorporation was studied. When cells were incubated with 6, 3, and 1.5 μg/ml of the conjugated protein, 70%, 50%, and 30% of cells were positive for the incorporated GFP, respectively (data not shown). The time-course analysis was next carried out using 3 μg/ml of the conjugated protein. The incorporation of peptide-conjugated GFP was observed within 2 h after treatment (Fig. 2B). About 30% of cells were positive for the protein (Fig. 2C, upper right panel). Then, about 50% of cells were positive for the incorporated GFP in 4 or 8 h (Fig. 2B, lower panels), indicating that most of the C45D18-dependent incorporation of conjugated protein was complete within several hours.

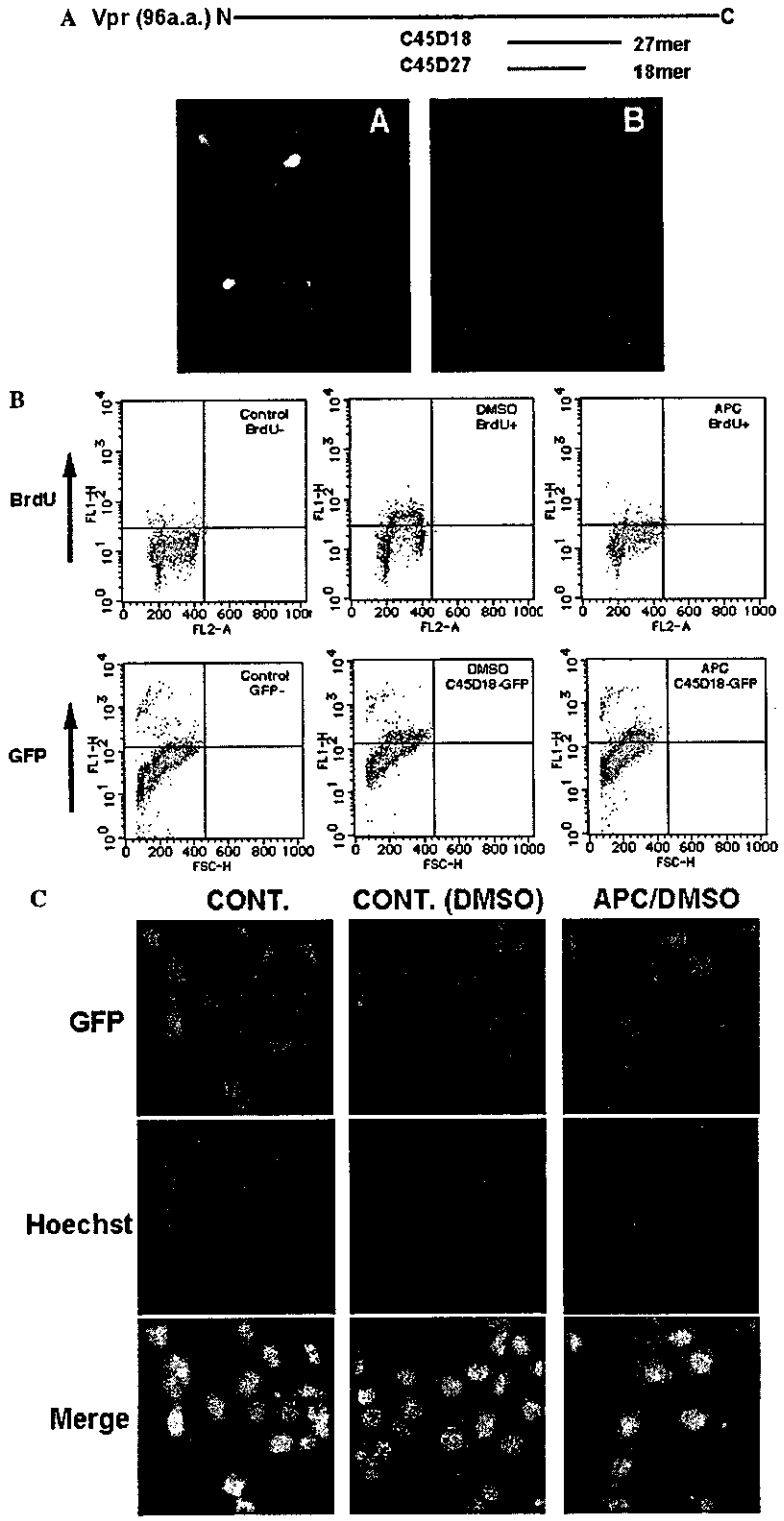

Fig. 3. Characterization of C45D18-dependent incorporation of GFP. (A) Incorporation of C45D18 into resting cells. HT1080 cells were arrested by serum-starvation for 4 days and then C45D18 or C47D27 was treated for about 12 h. Cell cycle arrest was confirmed by BrdU incorporation, followed by FACS analysis (data not shown). The incorporated peptides were detected with SA-FITC. Note that only C45D18 was incorporated into cells. (B) Incorporation of C45D18-conjugated GFP into resting cells. HL-60 cells were treated for 14 h with 1 μg/ml aphidicolin (APC), and then 3 μg/ml C45D18-conjugated GFP was treated for 5 h. Upper and lower panels show results of cell cycle analysis and incorporated GFP, respectively. As a control, cells were treated with DMSO, used as a solvent of APC (middle panels). After APC treatment, cells did not incorporate BrdU (upper right panel), but the incorporated GFP was detected in these cells (lower right panel). (C) Incorporation of C45D18-GFP into nucleus even under cell cycle arrest. HT1080 cells were treated for 14 h with 1 μg/ml APC and incubated with the conjugated GFP. The incorporated GFP was analyzed by laser-scanning microscopy. Results of C45D18-GFP added to control cells (left panels), DMSO-treated cells (middle panels), and APC-treated cells (right panels) are shown. Positive signals of the incorporated GFP (upper panels). DNA stained by Hoechst 33258 (middle panels), and merged images (lower panels) are shown.

It has been proposed that Tat, another accessory gene product of HIV-1, has a sequence of 9-mer aa with trafficking activity [20]. To compare the activity of C45D18 and Tat peptides, GFP was conjugated with each peptide at the same molar ratio (10:1) by the same procedure with C45D18. Then each protein was added to the culture media of two human cell lines, HL-60 and Jurkat cells. As shown in Fig. 2D, GFP conjugated with Tat peptide was not efficiently incorporated (blue), compared to the C45D18 (orange). In the present work, we conjugated peptides with protein through maleimide molecules and then directly added them to the culture medium without denaturing conjugated proteins. Since it is reported that Tat activity to transduce proteins is observed only after denaturing proteins [23], it may be possible that Tat activity of protein transduction is possibly detected after denaturing molecules.

It has been reported that Vpr has an activity to form channels in the cytoplasmic membrane [16,17], by which Vpr might be incorporated into cells. To exclude the possibility that trafficking of exogenous proteins is due to passive incorporation through membrane channels formed by Vpr-derived peptide, we added C45D18 and unconjugated GFP simultaneously, and then evaluated whether GFP was detected in the treated cells. No incorporated signals were observed (data not shown), indicating that C45D18 was active for transducing protein, only when it was conjugated with macromolecule.

Trafficking molecules into resting cells

It has been proposed that Vpr is responsible for infection of HIV to resting macrophages [6]. To know whether C45D18 could be incorporated into resting cells, HT1080 cells were first cultured for 4 days in FCS-free medium and then incubated with the peptide. FACS analysis on BrdU-positive cells clearly indicated that cells were not S-phase (data not shown). When C45D18 was treated with these cells, the peptide was again efficiently incorporated (Fig. 3A-A). By contrast, C45D28, a smaller peptide, was not incorporated at all (Figs. 3A and B), indicating that the incorporation of C45D18 was not due to the passive transport of small molecules into

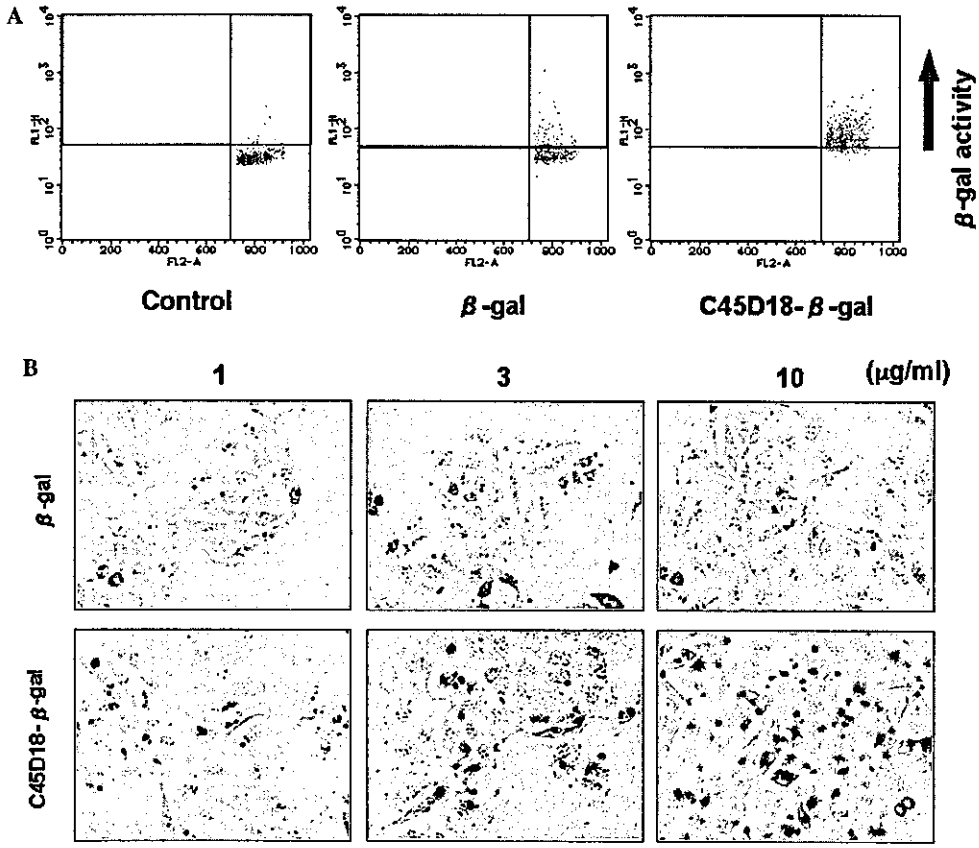

Fig. 4. Incorporation of bioactive molecule of C45D18. (A) Nuclear trafficking of active β-gal into adherent cells. HT1080 cells were treated overnight with control β-gal (upper panels) or C45D18-conjugated β-gal (lower panels). Then X-gal staining was carried out. Doses of treated proteins were 1 (left panels), 3 (middle panels), and 10 (right panels) μg/ml, respectively. β-Gal activity is indicated as black spots. Note that signals of β-gal activity are observed in regions corresponding to nucleus. (B) Incorporation of β-gal into CBMN cells by C45D18. CBMN cells were treated with C45D18-conjugated β-gal, and the activity of β-gal was detected by FACS analysis with a FluoReporter lacZ Flow Cytometry kit. Results of control (left panel), β-gal (middle panel), and β-gal conjugated with C45D18 (right panel) are shown.

cells. We next studied whether C45D18-conjugated protein was also incorporated into resting cells. HL-60 cells were first treated for 14 h with 1 μg/ml APC and then incubated for another 5 h with 3 μg/ml C45D18-conjugated GFP. We confirmed that cell cycle was completely arrested, as judged by incorporation of BrdU (Fig. 3B, upper right panel). Even under such condition, more than 50% of cells were positive for incorporated GFP (Fig. 3B, lower right panel). The same experiment was carried out on HT1080 cells and consistent results were obtained (Fig. 3C). Incorporation of C45D18-conjugated GFP into APC-treated cells was observed at almost the same level with control (Fig. 3D, right panels). Interestingly, the incorporated GFP was again detected in nuclear regions, judged by laser-scanning microscopy (Fig. 3C, middle and right panels). These data indicate that the nuclear trafficking of protein by C45D18 was not dependent on cellular growth.

Nuclear trafficking of bioactive macromolecules

To know whether C45D18 could transport a bioactive macromolecule, β-gal with a molecular weight of 465 kDa was conjugated with C45D18 and then added to cells. To show bioactivity, X-gal staining was carried out on the next day. As shown in Fig. 4A, β-gal activity was clearly detected in HT1080 cells treated with conjugated β-gal. The numbers of cells positive for of X-gal staining increased in a dose-dependent manner of treated β-gal (Fig. 4A). We also observed that β-gal activity was present in regions corresponding to nucleus.

C45D18-dependent incorporation of β-gal activity was also demonstrated by FACS analysis on CBMN cells that were treated with the protein (see Materials and methods). As shown in Fig. 4B, more than 90% of treated cells were positive for β-gal activity (Fig. 4B, right panel). By contrast, treatment of β-gal alone did not increase the number of cells positive for the activity (Fig. 4B, middle panel). These data indicate that the trafficking property by C45D18 can transduce bioactive molecule at high efficiency.

Discussion

In the present study, we identified a sequence encompassing 52–78 aa of Vpr (C45D18) as a novel PTD. To confirm the reproducibility of our observations, we synthesized C45D18 more than three times and examined the activity of the peptide conjugated with proteins. Independent experiments revealed that C45D18 or its conjugated proteins, when added to culture medium of cells, were efficiently incorporated into the nuclear region.

For nuclear trafficking of proteins into cells from outside, there are at least two steps where C45D18 should function. One is that C45D18 enables conjugated proteins to cross biomembranes, and another step is that C45D18 translocates the incorporated protein to the nucleus. Although the precise mechanism remains to be clarified, it has been well proposed that Vpr enters cells [7,13], when added to the culture medium. As a possible explanation of this phenomenon, it has been proposed that Vpr forms ion channels in cellular membranes [16,17]. The region responsible for channel formation has been recognized in amino-terminal 40 aa [17]. Crossing cellular membranes by the C45D18 would not, however, be due to the ion channel formation by a proposed region, since C45D18 is located in the C-terminal half of Vpr. How the conjugated protein enters cells remains to be clarified.

As one of the most important functions of Vpr, it is involved in the nuclear trafficking of a pre-integration complex of HIV-1 (PIC) [6,24], which explains an intriguing activity of HIV-1 to infect resting macrophages [25]. The mechanism of nuclear trafficking activity of Vpr has been extensively investigated, and it is well proposed that Vpr is a nucleopheric protein [6,24,26–28]. Interestingly, however, it does not have a classical nuclear localization signal. Although there are some controversial reports [8], it has been proposed that Vpr binds karyopherin α [6,24] and translocates PIC to the nucleus. Furthermore, Vpr has been shown to interact with members of nuclear pore complex (NPC) proteins such as Nsp1p [27] and nucleoporin hCG1 [28]. Functional analysis using chimeric proteins of Vpr and β-gal has indicated that two parts of Vpr promote nuclear trafficking of β-gal. It was reported that 71–96 aa of Vpr is still active in nuclear localization. Since C45D18 has a region of 53–78 aa, it might be possible that an overlapped region of 71–78 aa has an affinity to NPC proteins, responsible for nuclear trafficking. To know whether the overlapped region 71–78 aa of Vpr (peptide-8) functions for nuclear trafficking of C45D18, we added peptide-8 into culture medium of cells and compared with the properties of C45D18. Although we observed that C45D18 was incorporated into the nuclear region, but peptide-8 was scarcely translocated to nucleus (data not shown), implying that the region of 71–78 aa of Vpr is not enough for nuclear translocation of C45D18.

As an important observation, C45D18 could transduce exogenous molecules into resting cells. Although retrovirus gene transfer is frequently utilized in clinical fields, exogenous genes cannot be transduced in resting cells by the system. To circumvent this problem, modified lentiviral vectors are developed for transducing genes into resting cells [29]. On the other hand, recent observations reveal that a retroviral system occasionally results in fatal side effects [30], implying that a non-viral gene transfer system would be more reliable in future clinical use. In most of gene transfer systems, however, the expression of exogenous genes depends on break

down of nuclear membranes. To obtain an efficient gene expression in resting cells, it is crucial to develop a system by which exogenous genes are directly transferred into nucleus. Since C45D18 can efficiently translocate into the nucleus, it is tempting to speculate that the frequency of gene expression by non-viral gene transfer systems may be improved by the combination with C45D18.

It has been reported that several peptides derived from different sources—such as ANTP, herpes simplex VP22, and nine amino acids of Tat peptide-possess protein transduction activity. When compared to the activity of Tat, C45D18 has more potent activity in transporting molecules. It has been well proposed that the transduction activity of Tat requires protein denaturing [23]. Our present work reveals that C45D18 is more versatile than Tat peptide, since C45D18-conjugated molecules can be directly utilized for nuclear trafficking without any subsequent procedures. Additionally, C45D18 did not induce any cell-cycle abnormality or apoptosis (Fig. 1D), implying that it can be used without serious side effects.

Acknowledgments

We are grateful to Dr. Dovie Wylie for kind help with manuscript preparation. We also would like to express great thanks to IBL for technical help in conjugation of C45D18 and proteins. This work was supported by a Grant-in-Aid for Research on Human Genome, Tissue Engineering from the Ministries of Health, Labour and Welfare of Japan. This work was also partly supported by a research grant from the Rinsho Yakuri Research Foundation. Yoshiaki Osawa is a research resident supported by the Japanese Foundation for AIDS Prevention.

References

[1] F. Wong-Staal, P.K. Chanda, J. Ghrayeb, Human immunodeficiency virus: the eighth gene, AIDS Res. Hum. Retroviruses 3 (1987) 33–39.
[2] E.A. Cohen, R.A. Subbramanian, H.G. Göttlinger, Role of auxiliary proteins in retroviral morphogenesis, Curr. Top. Microbiol. Immunol. 214 (1996) 219–235.
[3] X.F. Yu, M. Matsuda, M. Essex, T.H. Lee, Open reading frame *vpr* of simian immunodeficiency virus encodes a virion-associated protein, J. Virol. 64 (1990) 5688–5693.
[4] W. Paxton, R.I. Connor, N.R. Landau, Incorporation of vpr into human immunodeficiency virus type 1 virions: requirement for the p6 region of *gag* and mutational analysis, J. Virol. 67 (1993) 7229–7237.
[5] E.A. Cohen, G. Dehni, J.G. Sodroski, W.A. Haseltine, Human immunodeficiency virus *vpr* product is a virion-associated regulatory protein, J. Virol. 64 (1990) 3097–3099.
[6] M.A. Vodicka, D.M. Koepp, P.A. Silver, M. Emerman, HIV-1 Vpr interacts with the nuclear transport pathway to promote macrophage infection, Genes Dev. 12 (1998) 175–185.
[7] P. Henklein, K. Bruns, M.P. Sherman, U. Tessmer, K. Licha, J. Kopp, C.M.C. de Noronha, W.C. Greene, V. Wray, U. Schubert, Functional and structural characterization of synthetic HIV-1 Vpr that transduces cells, localizes to the nucleus, and induces G2 cell cycle arrest, J. Biol. Chem. 275 (2000) 32016–32026.
[8] Y. Jenkins, M. McEntee, K. Weis, W.C. Greene, Characterization of HIV-1 vpr nuclear import: analysis of signals and pathways, J. Cell Biol. 143 (1998) 875–885.
[9] M. Shimura, Y. Tanaka, S. Nakamura, Y. Minemoto, K. Yamashita, K. Hatake, F. Takaku, Y. Ishizaka, Micronuclei formation and aneuploidy induced by Vpr, an accessory gene of human immunodeficiency virus type 1, FASEB J. 13 (1999) 621–637.
[10] M. Shimura, Y. Onozuka, T. Yamaguchi, K. Hatake, F. Takaku, Y. Ishizaka, Micronuclei formation with chromosome breaks and gene amplification caused by Vpr, an accessory gene of human immunodeficiency virus, Cancer Res. 59 (1999) 2259–2264.
[11] D.N. Levy, Y. Refaeli, R.R. MacGregor, D.B. Weiner, Serum Vpr regulates productive infection and latency of human immunodeficiency virus type 1, Proc. Natl. Acad. Sci. USA 91 (1994) 10873–10877.
[12] D.N. Levy, Y. Refaeli, D.B. Weiner, Extracellular Vpr protein increases cellular permissiveness to human immunodeficiency virus replication and reactivates virus from latency, J. Virol. 69 (1995) 1243–1252.
[13] M.-B. Huang, O. Weeks, L.-J. Zhao, M. Saltarelli, V.C. Bond, Effects of extracellular human immunodeficiency virus type 1 vpr protein in primary rat cortical cell cultures, J. Neurovirol. 6 (2000) 202–220.
[14] A. Kichler, J.C. Pages, C. Leborgne, S. Druillennec, C. Lenoir, D. Coulaud, E. Delain, E. Le Cam, B.P. Roques, O. Danos, Efficient DNA transfection mediated by the C-terminal domain of human immunodeficiency virus type 1 viral protein R, J. Virol. 74 (2000) 5424–5431.
[15] M.P. Sherman, U. Schubert, S.A. Williams, C.M.C. de Noronha, J.F. Kreisberg, P. Henklein, W.C. Greene, HIV-1 Vpr displays natural protein-transducing properties: implications for viral pathogenesis, Virology 302 (2002) 95–105.
[16] S.C. Piller, G.D. Ewart, A. Premkumar, G.B. Cox, P.W. Gage, Vpr protein of human immunodeficiency virus type 1 forms cation-selective channels in planar lipid bilayers, Proc. Natl. Acad. Sci. USA 93 (1996) 111–115.
[17] S.C. Piller, G.D. Ewart, D.A. Jans, P.W. Gage, G.B. Cox, The amino-terminal region of Vpr from human immunodeficiency virus type 1 forms ion channels and kills neurons, J. Virol. 73 (1999) 4230–4238.
[18] S. Console, C. Marty, C. Garcia-Echeverria, R. Schwendener, K. Ballmer-Hofer, Antennapedia and HIV transactivator of transcription (TAT) protein transduction domains promote endocytosis of high molecular weight cargo upon binding to cell surface glycosaminoglycans, J. Biol. Chem. 278 (2003) 35109–35114.
[19] G. Elliott, P. O'Hare, Intercellular trafficking and protein delivery by a herpesvirus structural protein, Cell 88 (1997) 223–233.
[20] N.J. Caron, Y. Torrente, G. Camirand, M. Bujold, P. Chapdelaine, K. Leriche, N. Bresolin, J.P. Tremblay, Intracellular delivery of a Tat-eGFP fusion protein into muscle cells, Mol. Ther. 3 (2001) 310–318.
[21] L. Yano, M. Shimura, M. Taniguchi, Y. Hayashi, T. Suzuki, K. Hatake, F. Takaku, Y. Ishizaka, Improved gene transfer to neuroblastoma cells by a monoclonal antibody targeting RET, a receptor tyrosine kinase, Hum. Gene Ther. 11 (2000) 995–1004.
[22] J. Sambrook, D.W. Russell, Molecular Cloning: A Laboratory Manual, Cold Spring Harbor Laboratory Press, Cold Spring Harbor, NY, 2001.
[23] M.C. Morris, J. Depollier, J. Mery, F. Heitz, G. Divita, A peptide carrier for the delivery of biologically active proteins into mammalian cells, Nat. Biotechnol. 19 (2001) 1173–1176.
[24] S. Popov, M. Rexach, G. Zybarth, N. Reiling, M.A. Lee, L. Ratner, C.M. Lane, M.S. Moore, G. Blobel, M. Bukrinsky, Viral protein R regulates nuclear import of the HIV-1 pre-integration complex, EMBO J. 17 (1998) 909–917.

[25] M.A. Vodicka, Determinants for lentiviral infection of non-dividing cells, Somat. Cell Mol. Genet. 26 (2001) 35–49.
[26] S. Popov, M. Rexach, L. Ratner, G. Blobel, M. Bukrinsky, Viral protein R regulates docking of the HIV-1 preintegration complex to the nuclear pore complex, J. Biol. Chem. 273 (1998) 13347–13352.
[27] R.A.M. Fouchier, B.E. Meyer, J.H.M. Simon, U. Fischer, A.V. Albright, F. Gonzalez-Scarano, M.H. Malim, Interaction of the human immunodeficiency virus type 1 Vpr protein with the nuclear pore complex, J. Virol. 72 (1998) 6004–6013.
[28] E. Le Rouzic, A. Mousnier, C. Rustum, F. Stutz, E. Hallberg, C. Dargemont, S. Benichou, Docking of HIV-1 Vpr to the nuclear envelope is mediated by the interaction with the nucleoporin hCG1, J. Biol. Chem. 277 (2002) 45091–45098.
[29] F. Galimi, I.M. Verma, Opportunities for the use of lentiviral vectors in human gene therapy, Curr. Top. Microbiol. Immunol. 261 (2002) 245–254.
[30] E. Marshall, Gene therapy. Second child in French trial is found to have leukemia, Science 299 (2003) 320.

Binding of 14-3-3β but not 14-3-3σ controls the cytoplasmic localization of CDC25B: binding site preferences of 14-3-3 subtypes and the subcellular localization of CDC25B

Sanae Uchida[1], Akiko Kuma[1,*], Motoaki Ohtsubo[2], Mari Shimura[3], Masato Hirata[4], Hitoshi Nakagama[5], Tsukasa Matsunaga[6], Yukihito Ishizaka[3] and Katsumi Yamashita[1,‡]

[1]Division of Life Science, Graduate School of Natural Science and Technology, Kanazawa University, Kakuma-machi, Kanazawa, 920-1192, Japan
[2]Institute of Life Science, Kurume University, Aikawa 2432-3, Kurume, 839-0861, Japan
[3]Division of Intractable Disease, International Medical Center of Japan, 21-1 Toyama 1-chome, Shinjuku-ku, Tokyo, 162-8655, Japan
[4]Laboratory of Molecular and Cellular Biochemistry, Faculty of Dental Science, and Station for Collaborative Research, Kyushu University, Maidashi, Fukuoka, 812-8582, Japan
[5]Biochemistry Division, National Cancer Center Research Institute, 1-1 Tsukiji 5-chome, Chuo-ku, Tokyo, 104-0045, Japan
[6]Laboratory of Molecular Human Genetics, Faculty of Pharmaceutical Sciences, Kanazawa University, 13-1 Takara-machi, Kanazawa, 920-0934, Japan

*Present address: Department of Cell Biology, National Institute for Basic Biology, 38 Nishigonaka, Myodaiji, Okazaki, 444-8585, Japan
‡Author for correspondence (e-mail: katsumi@kenroku.kanazawa-u.ac.jp)

Accepted 7 January 2004
Journal of Cell Science 117, 3011-3020 Published by The Company of Biologists 2004
doi:10.1242/jcs.01086

Summary

The dual specificity phosphatase CDC25B positively controls the G2-M transition by activating CDK1/cyclin B. The binding of 14-3-3 to CDC25B has been shown to regulate the subcellular redistribution of CDC25B from the nucleus to the cytoplasm and may be correlated with the G2 checkpoint. We used a FLAG-tagged version of CDC25B to study the differences among the binding sites for the 14-3-3 subtypes, 14-3-3β, 14-3-3ε and 14-3-3σ, and the relationship between subtype binding and the subcellular localization of CDC25B. All three subtypes were found to bind to CDC25B. Site-directed mutagenesis studies revealed that 14-3-3β bound exclusively near serine-309 of CDC25B1, which is within a potential consensus motif for 14-3-3 binding. By contrast, 14-3-3σ bound preferentially to a site around serine-216, and the presence of serine-137 and -309 enhanced the binding. In addition to these binding-site differences, we found that the binding of 14-3-3β drove CDC25B to the cytoplasm and that mutation of serine-309 to alanine completely abolished the cytoplasmic localization of CDC25B. However, co-expression of 14-3-3σ and CDC25B did not affect the subcellular localization of CDC25B. Furthermore, serine-309 of CDC25B was sufficient to produce its cytoplasmic distribution with co-expression of 14-3-3β, even when other putative 14-3-3 binding sites were mutated. 14-3-3ε resembled 14-3-3β with regard to its binding to CDC25B and the control of CDC25B subcellular localization. The results of the present study indicate that two 14-3-3 subtypes can control the subcellular localization of CDC25B by binding to a specific site and that 14-3-3σ has effects on CDC25B other than the control of its subcellular localization.

Key words: CDC25B, 14-3-3β, 14-3-3σ, Subcellular localization, G2 checkpoint

Introduction

The CDK (cyclin-dependent kinase) family of proteins controls the eukaryotic cell cycle, and one of these proteins, CDK1, is required for the onset and maintenance of mitosis. The activities of CDK family proteins related to cell cycle control are regulated by associations with cyclin proteins, interactions with cyclin-dependent kinase inhibitors, such as p21 and p27, and the phosphorylation-dephosphorylation cycle of CDK (Morgan, 1997). For instance, the phosphorylation of CDK1 at threonine-14 and tyrosine-15 by Wee1 and/or Myt1 kinases negatively controls CDK1 activity, whereas the dephosphorylation of CDK1 by the CDC25 family phosphatases activates CDK1, an essential step in the transition from G2 to M phase. The CDC25 family of dual protein phosphatases consists of three members, CDC25A, CDC25B, and CDC25C (Nilsson and Hoffman, 2000). CDC25A is thought to regulate the G1 to S transition, and CDC25B and C have been proposed to activate the CDK1/cyclin B1 complex to advance the cell cycle from G2 to M. Recent reports strongly suggest that CDC25A also has a function that is essential for the entry into and maintenance of M phase (Mailand et al., 2002).

The 14-3-3 family of proteins consists of small, acidic, highly conserved proteins that are present in all eukaryotic cells from yeast to mammals. There are seven isotypes present in mammalian cells. The 14-3-3 proteins are involved in numerous cellular processes related to signal transduction (Muslin and Xing, 2000; Tzivion et al., 2001; Yaffe, 2002).

These molecules bind to phosphoproteins at specific sequence motifs, which contain phosphoserine/threonine residues three amino acids downstream of an arginine (RxxS/T), and thereby regulate extracellular signaling or stress response pathways (Muslin et al., 1996; Yaffe et al., 1997). Emerging evidence suggests that 14-3-3 proteins are key regulators of cell cycle control, especially at cell cycle checkpoints, where they might function as negative regulators of DNA damage checkpoints. For example, one canonical 14-3-3 binding motif, which contains a phosphorylated serine residue, is similar to the consensus substrate motif of the checkpoint kinase Chk1 (Sanchez et al., 1997; Hutchins et al., 2000). In fission yeast, the 14-3-3 proteins Rad24/25 are required for checkpoint responses and are essential for cell survival (Ford et al., 1994). One of the 14-3-3 isotype proteins, 14-3-3σ is strongly up-regulated following genotoxic stress and is a downstream target of the tumor suppressor p53 (Hermeking et al., 1997).

The involvement of 14-3-3 in the progression from G2 to M was first suggested by the interactions of isolated 14-3-3β and ε with CDC25B (and CDC25A) and of isolated 14-3-3ζ with Wee1 (Conklin et al., 1995; Honda et al., 1997). Accumulated circumstantial evidence indicates that 14-3-3 negatively controls the G2-M transition by binding to these regulators. An association of 14-3-3 with human CDC25C was detected in G1, S and G2 phases, but not in M phase (Peng et al., 1997). The binding of 14-3-3 requires the Ser216 of CDC25C, and mutating this residue to Ala abolishes the interaction. This site is present in the potential recognition motif for 14-3-3 and is phosphorylated *in vitro* by checkpoint kinases, such as Chk1 and Chk2 (Sanchez et al., 1997; Peng et al., 1998; Matsuoka et al., 1998; O'Neill et al., 2002). Studies of the interaction between *Xenopus* CDC25C and 14-3-3 clearly demonstrated that the binding of 14-3-3 masks the nuclear localization signal of CDC25C, thereby causing nuclear exclusion of the protein without affecting its phosphatase activity (Kumagai et al., 1998; Kumagai and Dunphy, 1999; Yang et al., 1999). By contrast, the binding of 14-3-3 to *Xenopus* Wee1, after Chk1 activation by DNA damage or by stalled replication, augments Wee1 tyrosine kinase activity for CDK1 (Wang et al., 2000; Lee et al., 2001; Rothblum-Oviatt et al., 2001). Thus, the association of 14-3-3 with target proteins could modulate cell cycle progression through different mechanisms such as subcellular localization and enzyme activity, depending on cellular signaling.

In the normal cell cycle, CDC25B accumulates only at G2 phase and is degraded when cells exit M phase (Nagata et al., 1991; Galaktionov and Beach, 1991; Sebastian et al., 1993; Lammer et al., 1998). Interestingly, the overexpression of CDC25B induces a mitotic catastrophe by prematurely activating CDK1/cyclin B1, indicating that CDC25B induces mitosis more efficiently than CDC25C (Karlsson et al., 1999). In addition, the exogenous expression of CDC25B can override the G2 DNA damage checkpoint, and CDC25B is expressed in certain tumors (Miyata et al., 2001). Therefore, CDC25B has been proposed to be a potential oncogene acting to abrogate the DNA damage checkpoint (Galaktionov et al., 1995; Ma et al., 1999; Yao et al., 1999). Subcellular localization of CDC25B can be controlled by its association with 14-3-3 at a specific site on CDC25B2 or B3, Ser323 and might contribute to stall the cell cycle at the G2 phase following DNA damage (Mils et al., 2000; Davezac et al., 2000; Forrest and Babrielli, 2001). Ser323 of CDC25B2 or CDC25B3 (the equivalent to Ser309 of CDC25B1) is a crucial residue in the consensus 14-3-3 binding motif, where it is phosphorylated by the stress kinase p38 (Bulavin et al., 2001).

In the present study, we have analyzed the binding site specificity of three 14-3-3 subtypes, 14-3-3β, ε, and σ. Our results indicate that the binding site of 14-3-3σ differs markedly from those of 14-3-3β and 14-3-3ε. Moreover, the interaction of 14-3-3β or 14-3-3ε, but not of 14-3-3σ with CDC25B drives CDC25B from the nucleus into the cytoplasm. The biological significance of our results is discussed.

Materials and Methods

Cell culture and transfection

HEK293 cells (ATCC number CRL-1573) and U2OS cells (ATCC number HTB-96) were cultured in Dulbecco's modified Eagle's medium (DMEM) (Sigma, USA) supplemented with 10% fetal bovine serum (FBS) (Invitrogen, USA), 100 units/ml penicillin and 10 μg/ml streptomycin. Transient transfections were performed with FuGENE6 (Roche Diagnostics, Germany). For immunoprecipitation, cells were typically seeded at 1.3×10^6 per well. After 24 hours, cells were co-transfected with 2.5 μg of FLAG-tagged CDC25B and 1.0 μg of myc-tagged 14-3-3 DNA. For the indirect immunofluorescence experiments, cells were plated at a lower density, 2.0×10^5 per well and transfected after 24 hours with 3.0 μg of CDC25B DNA and 1.5 μg 14-3-3 of DNA. Transfected cells were processed for immunoblotting, immunoprecipitation, or immunostaining 24 hours after transfection. Leptomycin B, an inhibitor of CRM1 (exportin1), was obtained from Minoru Yoshida (RIKEN, Wako, Japan) and was administered to cells at a dose of 20 ng/ml to induce the nuclear accumulation of CDC25B.

Plasmids and site-directed mutagenesis

The cDNA of human CDC25B (CDC25B1 subtype), a kind gift from H. Okayama (University of Tokyo, Japan), was subcloned into the pEF6B vector (Invitrogen, USA) and expressed in transfected cells with a C-terminal FLAG tag. For point mutations at putative 14-3-3 binding sites, the following oligonucleotides (and their complements) were used to change serine to alanine (SA) in human CDC25B cDNA (CDC25B1). Clones with multiple mutations were generated by exchanging restriction fragments. The mutations were confirmed by sequencing.

S81A: 5′-CTGTCTCGACGGGCAGCCGAATCCTCCCTG-3′,
S137A: 5′-ATCAGACGCTTCCAGGCTATGCCGGTGAGG-3′,
S216A: 5′-GCCCAGAGACCCAGCGCGGCCCCCGACCTG-3′,
S309A: 5′-CTCTTCCGCTCTCCGGCCATGCCCTGCAGC-3′,
S361A: 5′-GTCCTCCGCTCAAAAGCACTGTGTCACGAT-3′.

The cDNAs of human 14-3-3β, ε, and σ were obtained by PCR amplification with the following oligonucleotides:

14-3-3β forward: 5′-ACTTGGAGTCAGCATATGACAATGGAT-3′,
14-3-3β reverse: 5′-CACTGGACGGATCCCAAAGCACGAGAA-3′,
14-3-3ε forward: 5′-GCCGCTGCCCATATGGATGATCGAGAG-3′,
14-3-3ε reverse: 5′-CTCTTGTGGGCGGATCCCTCACTGATT-3′,
14-3-3σ forward: 5′-GTCCCCAGACATATGGAGAGAGCCAGT-3′,
14-3-3σ reverse: 5′-GGTGGCGGGCAAGCTTCAGCTCTGGGG-CTC-3′.

PCR products were subcloned into the pEF6 vector. Each 14-3-3 cDNA was expressed in transfected cells in an N-terminal myc-tagged form.

Antibodies

Anti-FLAG M2 agarose was obtained from Sigma (USA). The rabbit

anti-FLAG antibody was described previously (Wang et al., 2001). Rabbit polyclonal and mouse monoclonal anti-myc-tag antibodies were purchased from Cell Signaling (USA). Antibodies to 14-3-3β (C-20), 14-3-3ε (T-16), and 14-3-3σ (N-14) were purchased from Santa Cruz Biotechnology (USA).

Preparation of crude cell extracts, immunoprecipitation and immunoblotting

Transfected cells were lysed in immunoprecipitation (IP) buffer (50 mM Tris-HCl pH 7.5, 150 mM NaCl, 0.5% NP-40, 5 mM EGTA, 1 mM EDTA) supplemented with a protease inhibitor mix and a phosphatase inhibitor mix. The protease inhibitor mix contained a 1:100 dilution of FOCUS protease arrest (Calbiochem, USA), 5 μg/ml E64 (Roche Diagnostics, Germany), 0.4 μM cathepsin inhibitor III (Sigma, USA), 10 μM MG132 (Calbiochem, USA), 20 μM N-acetyl-leu-leu-norleu-ala (Sigma, USA) and 1 mg/ml Pefabloc®SC (Roche Diagnostics, Germany). The phosphatase inhibitor mix consisted of a 1:100 dilution of Phosphatase inhibitor cocktail II (Sigma, USA), 20 mM *p*-nitrophenyl phosphate, 20 mM NaF, 20 mM β-glycerophosphate, 0.2 μM microcystin-LR (Calbiochem, USA), 0.2 μM calyculin A (Wako, Japan), 0.2 μM okadaic acid (Wako, Japan), 0.1 μM phenylarsin (Sigma, USA), and 0.2 μM cantharidin (Sigma, USA). FLAG-tagged CDC25B and mutant proteins were immunoprecipitated using FLAG M2-agarose; myc-tagged 14-3-3 proteins were immunoprecipitated with mouse monoclonal anti-myc tag antibody followed by protein G-Sepharose (Amersham Bioscience, USA). Cell lysates and immunoprecipitates were analyzed on western blots using rabbit polyclonal anti-FLAG (for CDC25B) or anti-myc antibodies (for exogenous 14-3-3), or 14-3-3 subtype-specific antibodies (for endogenous 14-3-3).

Indirect immunofluorescence microscopy

Transfected HEK293 cells grown on glass coverslips were fixed in 3.7% formaldehyde in PBS and then permeabilized with 0.5% Triton X-100 in PBS. FLAG-tagged CDC25B and mutants were detected with rabbit polyclonal anti-FLAG antibody and Alexa-594-conjugated goat anti-rabbit IgG (Molecular Probes, USA). Alternatively, myc-tagged 14-3-3 proteins were detected with mouse monoclonal anti-myc-tag antibody and Alexa-488-conjugated goat anti-mouse IgG (Molecular Probes, USA). In all samples, DNA was visualized with 4′,6-diamidino-2-phenylindole (DAPI) (Sigma, USA) at 0.1 μg/ml. To quantify the subcellular localization of CDC25B, more than 200 transfectant cells were counted and classified as having nuclear, diffuse or cytoplasmic localization.

Results

Binding of 14-3-3β, ε, and σ to CDC25B

Several groups have reported the interaction of 14-3-3 isotypes, such as 14-3-3β, ε, η, and ζ, with CDC25B (Mils et al., 2000; Forrest and Gabrielli, 2001). We have isolated 14-3-3β and ε as proteins that interact with CDC25B in yeast two-hybrid screening (S.U., A.K., M.O., M.S., M.H., H.N., T.M., Y.I. and K.Y., unpublished data), obtaining the same results as those previously reported (Conklin et al., 1995). Apart from these two 14-3-3 proteins (β and ε), 14-3-3σ was also reported to be possibly involved in a DNA damage checkpoint (Hermeking et al., 1997; Chan et al., 1999, 2000), which prompted us to isolate its cDNA and analyze its interaction with CDC25B.

We expressed FLAG-tagged CDC25B with myc-tagged 14-3-3β, ε or σ in HEK293 or U2OS cells and examined their interaction (Fig. 1). Expression of these proteins was confirmed in cell extracts prepared from transfected cells, as shown in Fig. 1 (Lysate). CDC25B was immunoprecipitated with anti-FLAG beads followed by western blotting and detection with either anti-FLAG or anti-myc antibody to detect CDC25B bound to 14-3-3. The results in Fig. 1 (IP: CDC25B) clearly indicate that all three 14-3-3 proteins can bind to CDC25B in co-transfected cells. To further confirm these results, reciprocal immunoprecipitation and western blot experiments were conducted in which CDC25B was detected in anti-myc immunoprecipitates of 14-3-3β, ε, or σ (Fig. 1, IP: 14-3-3). Thus, 14-3-3σ was most probably a new CDC25B-interacting protein.

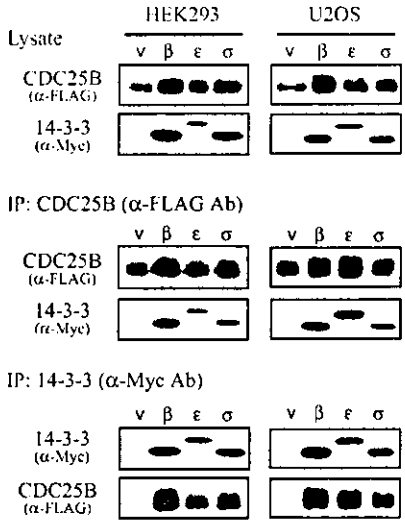

Fig. 1. 14-3-3β, 14-3-3ε, and 14-3-3σ bind to CDC25B in transfected cells. HEK293 (left panels) or U2OS (right panels) cells were transfected with FLAG-tagged CDC25B together with either empty vector or one of the myc-tagged 14-3-3 subtypes as described in Materials and Methods. (Top row) Lysate. Expression of CDC25B and 14-3-3- subtypes was confirmed in cell lysates with anti-FLAG antibody against CDC25B or anti-myc antibody against 14-3-3, respectively. (Middle row) IP: CDC25B (α-FLAG Ab). CDC25B was immunoprecipitated with anti-FLAG beads followed by western blotting and detection with anti-FLAG antibody to detect CDC25B and anti-myc antibody to detect CDC25B-bound 14-3-3. (Bottom row) IP: 14-3-3 (α-myc Ab. Reciprocal immunoprecipitation; CDC25B was detected in anti-myc immunoprecipitates. Protein 14-3-3 subtypes were immunoprecipitated with anti-myc antibody; the collected 14-3-3 or 14-3-3-bound CDC25B was detected by immunoblotting. v, empty vector; β, 14-3-3β, ε; 14-3-3ε, σ; 14-3-3σ.

Binding site specificity of 14-3-3 subtypes

The binding of 14-3-3 proteins to target proteins requires the specific motif RSxS/T(P)xP, where S/T(P) and x represent phosphoserine or phosphothreonine, and any amino acid, respectively (Muslin et al., 1996; Yaffe et al., 1997). The arginine (R) at position –3 from the phosphorylatable serine (or threonine) is a minimal requirement. In *Xenopus* for instance, after phosphorylation of CDC25 or Wee1 by Chk1 or other kinases, 14-3-3ε binds to the phosphorylated Ser287 in the RSPSMP sequence of CDC25 (Kumagai et al., 1998; Yang et al., 1999) and to the phosphorylated Ser549 in the RSVSFT sequence of Wee1 (Wang et al., 2000; Lee et al., 2001). There are several RxxS sites in CDC25B (or in our case, CDC25B1),

of which we chose the following five: 78-RRAS-81, 134-RFQS-137, 213-RPSS-216, 306-RSPS-309, and 358-RSKS-361, as shown in Fig. 2A. Of the relevant serine residues, Ser309 and Ser361 were phosphorylated by p38 in vitro and Ser309 was reported to be crucial for 14-3-3 binding after phosphorylation (Bulavin et al., 2001).

To analyze binding site specificity, we constructed three different groups of mutants in respect to the five above mentioned phosphorylatable serine sites of CDC25B1. Members of the first group have only a single mutation that changed one phosphorylatable serine to a non-phosphorylatable alanine; these mutants were namend CDC25B-S81A, S137A, etc. Members of the second group only remain a single phosphorylatable serine residue and contain mutations that changed the four serine residues to alanines; these mutants were named CDC25B-81S, 137S, etc. The only member of the last group is CDC25B-5SA in which all five serine residues were mutated to alanines. Using these mutants and the wild-type CDC25B, we determined the binding site specificity of 14-3-3β, ε, and σ.

Wild-type or mutant CDC25B were co-transfected with 14-3-3β, ε, or σ. Crude cell extracts were prepared, and expression of CDC25B and 14-3-3 was confirmed. Protein extracts were immunoprecipitated with anti-FLAG or anti-myc antibody, transferred for western blotting and detected with anti-myc or anti-FLAG antibody, respectively, to assess binding. We observed similar expression levels of CDC25B and 14-3-3 in transfected cells (Fig. 2B, Lysate), although lower levels of CDC25B mutants that failed to interact with 14-3-3, such as 81S and 5SA mutants, were occasionally detected (S.U., A.K., M.O., M.S., M.H., H.N., T.M., Y.I. and K.Y., unpublished data).

Interestingly, each 14-3-3 protein bound to a specific site on CDC25B (Fig. 2B, IP: CDC25B). These results clearly indicate that the CDC25B point mutation that changed Ser309 to Ala309, completely abolished 14-3-3β binding and that mutations of the other putative binding sites had essentially no effect on binding when compared with wild-type CDC25B. Also, experiments with the CDC25B mutant containing a single phosphorylatable serine revealed that Ser309 was the

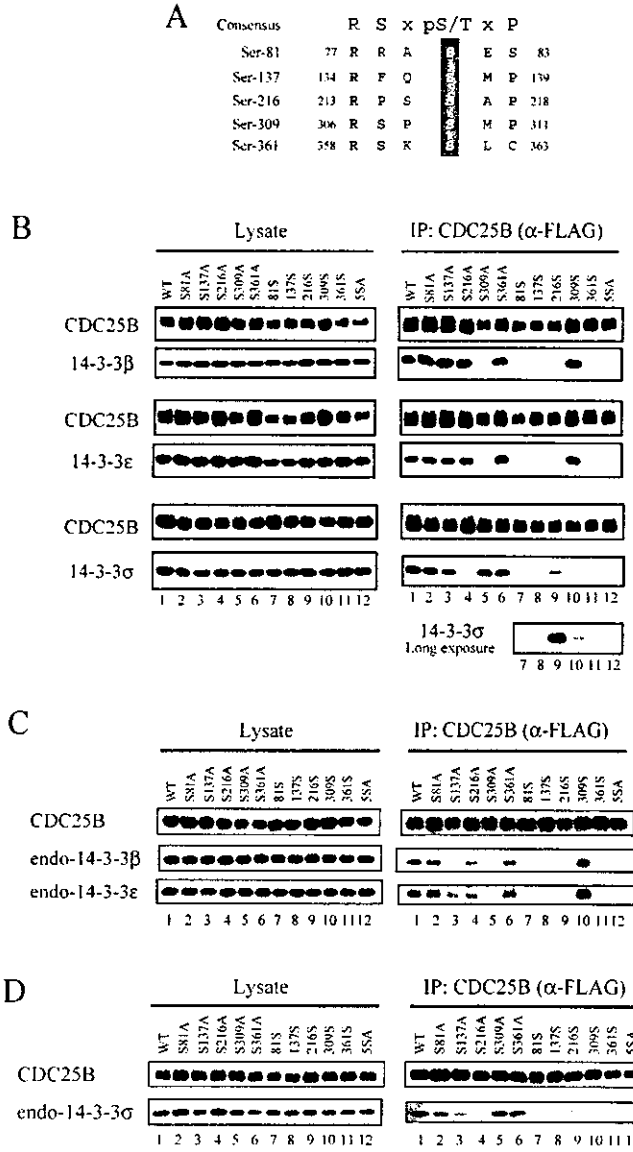

E

14-3-3	CDC25B mutants											
	WT	S81A	S137A	S216A	S309A	S361A	81S	137S	216S	309S	361S	5SA
14-3-3β	++	++	++	++	±	++	–	–	–	++	–	–
endo-14-3-3β	++	++	+	++	–	++	–	–	–	++	–	–
14-3-3ε	++	++	++	++	±	++	–	–	–	++	–	–
endo-14-3-3ε	++	++	+	+	±	++	–	–	–	++	–	–
14-3-3σ	++	++	++	–	++	++	–	–	+	–	–	–
endo-14-3-3σ	++	++	+	–	++	++	–	–	+	–	–	–

Fig. 2. Binding of 14-3-3 subtypes to CDC25B is site specific. (A) Putative 14-3-3 consensus binding sites in CDC25B. (B-D) Mutants of CDC25B were transfected into HEK293 or U2OS cells either alone or together with 14-3-3 subtypes as indicated. Recovered CDC25B proteins are indicated (upper panel of each set of figures). The letters at the top and numbers at the bottom of each blot represent the CDC25B mutants: wild-type (1); S81A (2); S137A (3); S216A (4); S309A (5); S361A (6); 81S (7); 137S (8); 216S (9); 309S (10); 361S (11); 5SA (12). The definitions of the abbreviations for each mutant are described in the text. (B) Mutants of CDC25B were co-transfected into HEK293 cells with 14-3-3 subtypes β, ε or σ. Protein expression was determined by immunoblot. Wild-type or mutant CDC25B proteins were immunoprecipitated with anti-FLAG beads, and CDC25B-bound 14-3-3 was determined in the lysate (Lysate) and the immunoprecipitate [IP: CDC25B (α-FLAG Ab)]. Separate panel 'long exposure' shows 14-3-3 subtype σ after an exposure for 1 hour. (C) Mutants of CDC25B were transfected into HEK293 cells. Recovered CDC25B proteins and CDC25B-bound endogenous 14-3-3β (endo-14-3-3β) or endogenous 14-3-3ε (endo-14-3-3ε) were detected with specific antibodies in the lysate (Lysate) and the immunoprecipitate [IP: CDC25B (α-FLAG Ab]. (D) Mutants of CDC25B were transfected into U2OS cells. Recovered CDC25B and CDC25B-bound endogenous 14-3-3σ (endo-14-3-3σ) were detected with specific antibodies in the lysate (Lysate) and the immunoprecipitate [IP: CDC25B (α-FLAG Ab].(E) Binding of endogenous and transfected 14-3-3 subtypes to CDC25B mutants. ++, well bound; +, detectably bound; ±, faintly bound (could be detected only after long exposure); –, no binding.

sole site responsible for 14-3-3β binding. A faint signal was detected with the CDC25B mutants containing Ser137 or Ser216, but only after a long exposure time (S.U., A.K., M.O., M.S., M.H., H.N., T.M., Y.I. and K.Y., unpublished data). Exactly the same results were obtained for 14-3-3ε binding (Fig. 2B), i.e. the intact Ser309 fulfills the binding requirement. Surprisingly, entirely different results were obtained when 14-3-3σ was co-expressed with CDC25B. As shown in Fig. 2B, the mutation of Ser309 to Ala309 had little effect on 14-3-3σ binding. Instead, a single mutation changing Ser216 to Ala216 apparently abrogated the binding of 14-3-3σ. Experiments with single-serine constructs of CDC25B provided complementary results, indicating that only Ser216 is responsible for 14-3-3σ binding. Notice, that the amount of 14-3-3σ that bound to the CDC25B-S216 mutant was roughly half the amount of 14-3-3β or ε that bound to the CDC25B-S309 mutant. Therefore, the affinity of 14-3-3σ for Ser216 seems to be lower than those of 14-3-3β and ε for Ser309. Furthermore, 14-3-3σ bound to two other binding sites, Ser137 and Ser309, although with a lower affinity than the binding to Ser216 (Fig. 2B, Long exposure).

Binding of endogenous 14-3-3 to CDC25B

Next, we addressed the question of whether endogenous 14-3-3 binds to transfected CDC25B. After transfection of wild-type or mutant CDC25B, CDC25B was recovered and CDC25-bound 14-3-3β, ε, or σ was detected with subtype-specific antibodies. CDC25B was transfected to HEK293 cells to investigate binding of 14-3-3β and ε. U2OS cells were used to determine 14-3-3σ binding because no expression of 14-3-3σ was detected in HEK293 cells. Binding of endogenous 14-3-3β and ε is shown in Fig. 2C and that of 14-3-3σ in Fig. 2D. As illustrated, the results were essentially the same as those for the exogenously expressed ones. 14-3-3β and ε preferentially bound to Ser309 and a mutation to Ala at this site impaired 14-3-3 binding. Unlike 14-3-3β and ε, a Ser to Ala mutation at Ser216 eliminated 14-3-3σ binding (summarized in Fig. 2E). As clearly indicated, both endogenous and exogenous 14-3-3β and ε preferentially bind to Ser309, whereas 14-3-3σ prefers Ser216. Besides these two sites, Ser137 seems to be a favored binding site for the three 14-3-3 subtypes tested here because the binding signals are reduced by mutation at Ser137 (Fig. 2C and D). In respect to the other putative binding sites, we found no evidence that the 14-3-3 subtypes bind to either Ser81 or Ser361.

Multiple binding sites for 14-3-3σ on CDC25B

The results shown in Fig. 2 suggest that 14-3-3σ binds to CDC25B at multiple sites and possibly requires two sites to stably bind the protein. To explore this further, we constructed a series of mutants in which two serine residues were changed to alanine, and examined the binding of the 14-3-3 subtypes (Fig. 3). Compared with the single SA mutant (i.e. S216A), binding of 14-3-3σ to double SA mutants, such as S216/309A, was weaker or absent. Further work with the double mutants indicated that either of two sites, Ser137 or Ser309, seem to work cooperatively with Ser216. These results strongly suggest that 14-3-3σ requires two sites, Ser216 and Ser137 or Ser216 and Ser309, to interact effectively with CDC25B, and that 14-3-3σ might function as a dimer.

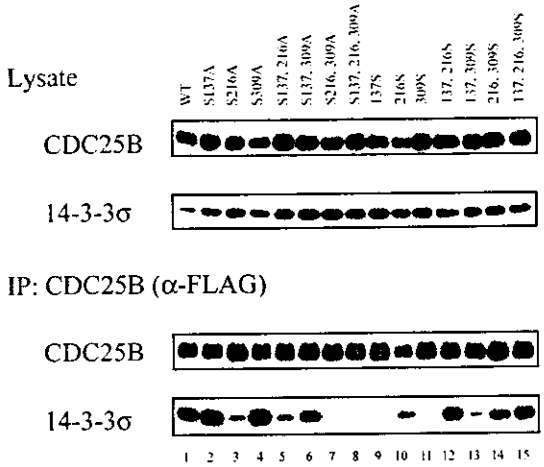

Fig. 3. Efficient binding of 14-3-3σ to CDC25B requires two independent sites. HEK293 cells were co-transfected with 14-3-3σ and a series of CDC25B mutants. Protein expression (Lysate) and protein binding (IP: CDC25B (α-FLAG Ab)) were detected. The letters in the upper panel of Lysate indicate CDC25B wild type and respective mutants. The definitions of the abbreviations for each mutant are described in the text.

14-3-3 binding sites and subcellular localization of CDC25B

Binding of 14-3-3 to CDC25B was previously reported to induce the redistribution of CDC25B from the nucleus to the cytoplasm; the amino acid residue essential for this effect was shown to be Ser323 of CDC25B3 (or CDC25B2), which corresponds to Ser309 of CDC25B1 in our experiments (Davezac et al., 2000; Forrest and Gabrielli, 2001). Therefore, we analyzed the subcellular localization of CDC25B mutants expressed in combination with 14-3-3 subtypes that possess different binding site preferences. To assess the effects of co-transfection on the subcellular localization of CDC25B, we distinguished three different distributions [nuclear (N), diffuse (N=C) and cytoplasmic (C)] of CDC25B (Fig. 4A). The localization of exogenously expressed CDC25B was mainly nuclear (Fig. 4B), transfected 14-3-3β or σ was detected in the cytoplasm (S.U., A.K., M.O., M.S., M.H., H.N., T.M., Y.I. and K.Y., unpublished data). Upon co-transfection with 14-3-3β, CDC25B exhibited a diffuse distribution (Fig. 4B). Quantitatively, the percentage of cells with nuclear CDC25B was reduced from 55% to 30% and that of cells with a diffuse distribution increased from 38% to 60% when co-expressed with 14-3-3β. Based on our results, it is possible that nuclear localization is disturbed by 14-3-3 binding. Interestingly, the expression of 14-3-3σ had no effect on the localization of CDC25B. These results led us to hypothesize that when 14-3-3β binds to Ser309 of CDC25B, it can drive CDC25B from the nucleus to the cytoplasm, but that 14-3-3σ, which does not bind primarily to Ser309, has no ability to do so.

Effects of mutations at 14-3-3 binding sites on the localization of CDC25B

The primary 14-3-3β binding site on CDC25B was Ser309, and a point mutation at this site that changed serine to alanine abolished the interaction. If the binding of 14-3-3β is correlated

with the cytoplasmic localization of CDC25B, 14-3-3β could not drive the CDC25B mutant out of the nucleus. The results shown in Fig. 4C indicate that the mutation Ser309 to Ala309 in CDC25B completely disrupted its cytoplasmic localization with more than 90% of the mutant protein being located in the nuclei. In contrast to the wild type, this CDC25B mutant was not diffused into the cytoplasm by co-expression of 14-3-3β or 14-3-3σ. However, mutant S216A behaved like the wild type, i.e. its subcellular localization was effectively changed from nuclear to diffuse when co-expressed with 14-3-3β (Fig. 4D). Moreover, introduction of 14-3-3σ did not cause any change in the distribution of CDC25B. Collectively, these results show that Ser309 is essential for the cytoplasmic distribution of CDC25B and that Ser216 does not have any influence on the subcellular localization of CDC25B, even when 14-3-3σ binds to it.

To confirm that the subcellular distribution of CDC25B by 14-3-3β depends on Ser309, we made mutants in which serine was changed to alanine at four of the five sites that have a single phosphorylatable serine residue. The mutants were denoted as CDC25B-81S, CDC25B-137S, CDC25B-216S, CDC25B-309S and CDC25B-361S (as mentioned in Fig. 2). These CDC25B mutants were transfected with or without 14-3-3 and their localizations analyzed. Only CDC25B-309S behaved like the wild type (Fig. 5B); the other mutants exhibited nuclear localizations, probably because they possessed the S309A mutation and could not bind to 14-3-3β (Fig. 5A). Wild-type CDC25B and the CDC25B-309S mutant exhibited nuclear localization in about 60% of the cells (Fig. 5B). As was the case with wild-type CDC25B (see Fig. 4B), the expression of 14-3-3β antagonized the nuclear localization of CDC25B-309S and led to a diffuse distribution (Fig. 5B). In contrast to 14-3-3β, 14-3-3σ did not bind to the mutant and had no effect on the nuclear localization of CDC25B-309S or wild-type CDC25B (Fig. 5B). These results strongly suggest that only Ser309 of CDC25B is required for the control of the subcellular localization of CDC25B by 14-3-3β.

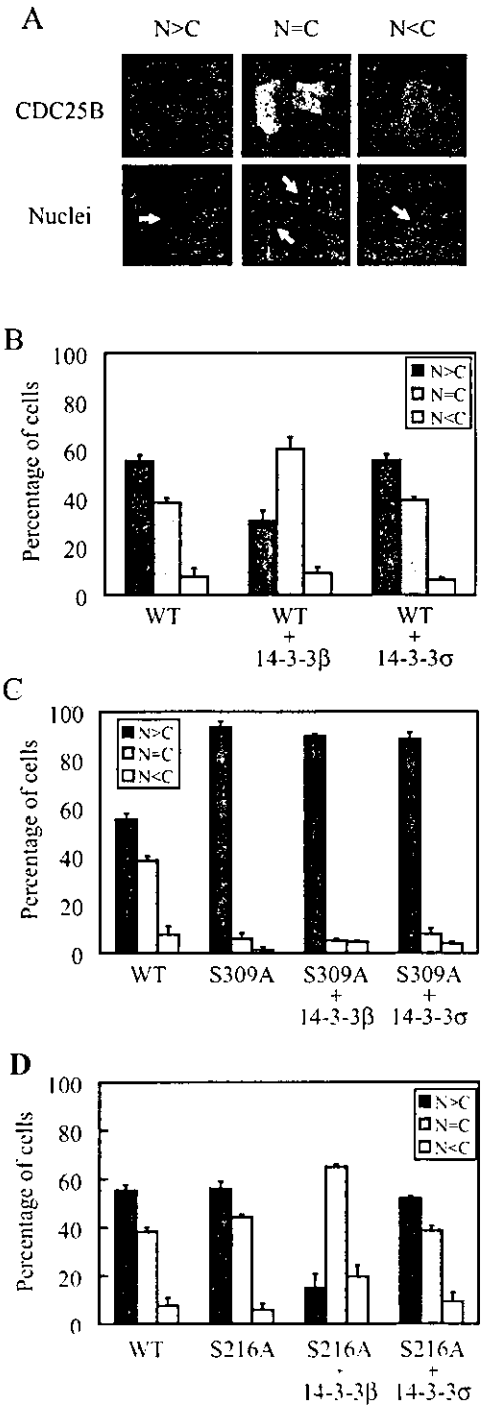

Effects of 14-3-3ε on the nuclear localization of CDC25B

The results shown in Fig. 2 indicate that Ser309 of CDC25B is the specific binding site for 14-3-3ε. We examined the effects

Fig. 4. 14-3-3β but not 14-3-3σ efficiently redistributes CDC25B from the nucleus to the cytoplasm. HEK293 cells were transfected with FLAG-tagged CDC25B in combination with empty vector, myc-tagged 14-3-3β or myc-tagged 14-3-3σ, followed by immunostaining with anti-FLAG antibodies to detect the subcellular localization of CDC25B and with anti-myc antibodies to detect co-transfected 14-3-3 proteins. Analyses showed that more than 95% of the cells that expressed CDC25B also expressed the co-transfected 14-3-3 proteins. (A) Exemplary images, showing how the subcellular distribution of CDC25B was evaluated: N>C, predominantly nuclear; N=C diffuse; N<C, predominantly cytoplasmic. (B) Wild-type CDC25B was co-transfected with empty vector (WT), myc-tagged 14-3-3β (WT+14-3-3β) or myc-tagged 14-3-3σ (WT+14-3-3σ) to quantify the subcellular distribution of CDC25B. Over 200 cells expressing CDC25B were counted to determine the percentage of cells that express CDC25B with nuclear, diffuse and cytoplasmic distribution. Error bars in graphs represent the means±s.d. of three independent experiments. (C) Transfection with wild-type CDC25B alone (WT), S309A mutant of CDC25B alone (S309A) and mutant S309A in combination with myc-tagged 14-3-3β (S309A+14-3-3β) or myc-tagged 14-3-3σ (S309A+14-3-3σ). Over 200 cells expressing CDC25B were counted to determine the percentage of cells that express CDC25B with nuclear, diffuse and cytoplasmic distribution. Error bars in graphs represent the means±s.d. of three independent experiments. (D) Transfection with wild-type CDC25B alone (WT), S216A mutant of CDC25B alone (S216A) and mutant S216A in combination with myc-tagged 14-3-3β (S216A+14-3-3β) or myc-tagged 14-3-3σ (S216A+14-3-3σ). Over 200 cells expressing CDC25B were counted to determine the percentage of cells that express CDC25B with nuclear, diffuse and cytoplasmic distribution. Error bars in graphs represent the means±s.d. of three independent experiments.

of 14-3-3ε on the subcellular localization of CDC25B in three sets of experiments. First, 14-3-3ε was co-transfected with wild-type CDC25B and CDC25B-distribution (as defined above and in Fig. 4A) was analyzed by counting the cells. Co-expression of 14-3-3ε reduced the percentage of cells with nuclear localization of CDC25B from 55% to 47% and concomitantly increased the percentage of cells displaying a diffuse pattern from 40% to 55% (Fig. 6A). Second, 14-3-3ε was co-transfected with the CDC25B-309S mutant. Here, the nuclear localization of CDC25B decreased from 60% to 37%, whereas its diffuse distribution increased from 35% to 55% (Fig. 6B). We found no effects of the co-expression of 14-3-3ε on the subcellular localization of the CDC25B-S309A mutant (Fig. 6C). In summary, the results with 14-3-3ε were exactly the same as those obtained with 14-3-3β and different from those with 14-3-3σ.

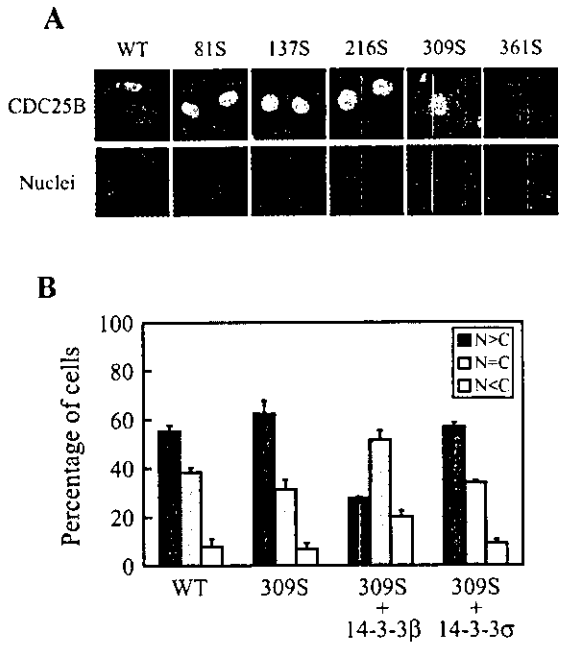

Fig. 5. Only the 309S mutant of CDC25B was distributed diffusely with co-transfection of 14-3-3β. (A) Wild type CDC25B or different CDC25B mutants with a single phosphorylatable serine were co-transfected with 14-3-3β into HEK293 cells. (Upper panels) Subcellular localization of CDC25B wild type and mutants. (Lower panel) Corresponding images of nuclei. (B) Percentage of cells transfected with mutant CDC25B 309S (shown in A) that express CDC25B with nuclear, diffuse and cytoplasmic distribution. Over 200 cells expressing CDC25B were counted to determine the percentage of cells that express CDC25B. Transfection with wild-type CDC25B alone (WT), 309S mutant of CDC25B alone (309S) and mutant 309S in combination with myc-tagged 14-3-3β (309S +14-3-3β) or myc-tagged 14-3-3σ (309S +14-3-3σ). Error bars in graphs represent the means±s.d. of three independent experiments. Subcellular distribution of CDC25B: N>C, predominantly nuclear; N=C diffuse; N<C, predominantly cytoplasmic (C).

Effects of 14-3-3β binding on the nuclear import of CDC25B

Several previous studies demonstrated that treating cells with leptomycin B (LMB), a CRM1 (exportin1) inhibitor, disrupts the cytoplasmic localization of CDC25B (Nishi et al., 1994; Kudo et al., 1998; Karlsson et al., 1999; Davezac et al., 2000) (Fig. 7A). Therefore, it might be that 14-3-3β-binding slows down the nuclear import of CDC25B by LMB. After transfecting CDC25B with or without 14-3-3β, cells were treated with LMB and the nuclear accumulation of CDC25B was measured. As shown in Fig. 7B, co-expression of exogenous 14-3-3β efficiently inhibited the nuclear import of CDC25B. Notice that this effect was not observed when 14-3-3σ was co-transfected with CDC25B. These results suggest that 14-3-3β masks the nuclear localizing signal (NLS) of CDC25B, which is located about 30 amino acids downstream of Ser309.

Discussion

It has long been believed that higher eukaryotic cells have two dual specificity phosphatases, CDC25B and CDC25C, which activate CDK1/cyclin B to initiate mitosis. Recent reports indicate that another dual specificity phosphatase, CDC25A, plays a crucial role in G2-M events (Mailand et al., 2002). CDC25A can bind and activate CDK1/cyclin B, and downregulation by RNAi delays mitotic entry. In addition, the overexpression of CDC25A abrogates the G2 DNA-damage checkpoint (Mailand et al., 2002; Chow et al., 2003). Therefore, it is possible to regard CDC25A as a master activator of CDK/cyclin in the cell cycle, and the roles of

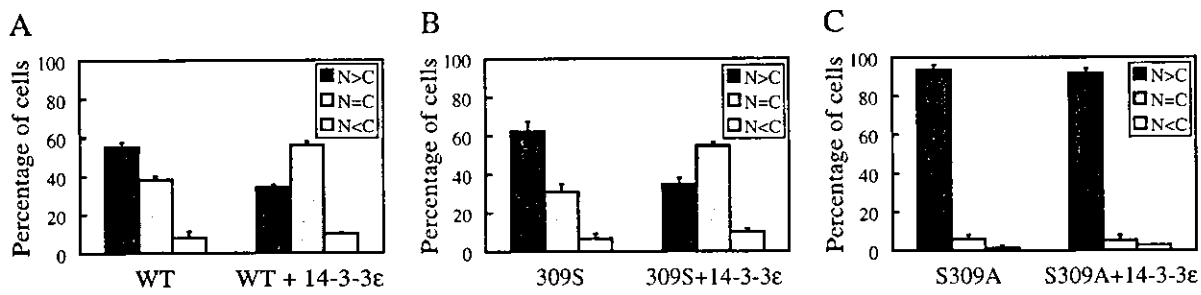

Fig. 6. 14-3-3ε had effects similar to those of 14-3-3β on the subcellular localization of CDC25B. HE293 cells were transfected with (A) wild-type CDC25B, (B) the 309S mutant or (C) the S309A mutant with or without 14-3-3ε. Over 200 cells expressing CDC25B were counted to determine the percentage of cells that express CDC25B with nuclear, diffuse and cytoplasmic distribution. Error bars in graphs represent the means±s.d. of three independent experiments. Subcellular distribution of CDC25B: N>C, predominantly nuclear; N=C diffuse; N<C, predominantly cytoplasmic (C).

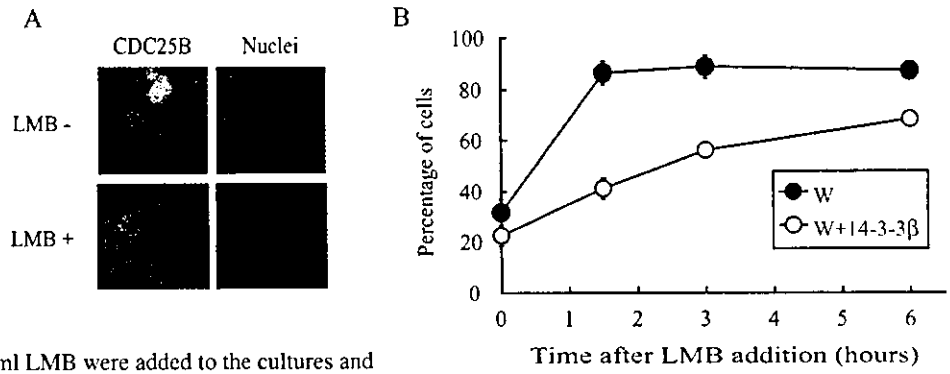

Fig. 7. Binding of 14-3-3β to CDC25B efficiently slowed down the nuclear import of CDC25B induced by leptomycin B (LMB). (A) HEK293 cells transfected with wild-type CDC25B and treated with 20 ng/ml LMB at for 3 hours. Transfected CDC25B was detected with anti-FLAG antibody. The upper and lower panels show the results without or with LMB treatment, respectively. (B) HEK293 cells transfected with wild-type CDC25B alone or with 14-3-3β. Twenty-four hours after transfection, 20 ng/ml LMB were added to the cultures and the percentage of cells exhibiting nuclear-specific localization of CDC25B was determined at the indicated time-points: 0 (before addition of LMB), 1.5, 3 or 6 hours after the addition. Over 200 cells expressing CDC25B were counted to determine the percentage of cells that express CDC25B. The percentage of cells with a nuclear localization (as shown in Fig. 4) was determined from three independent experiments. ●, CDC25B; ○,CDC25B with 14-3-3β.

CDC25B and CDC25C as being restricted to G2-M events to activate CDK1/cyclin B.

It has been proposed that CDC25C inhibits human CDC25C, by downregulating its phosphatase activity or by binding 14-3-3 after the phosphorylation of Ser216 (Peng et al., 1997; Blasina et al., 1999; Furnari et al., 1999; Graves et al., 2001). The amount of cellular CDC25C is essentially kept constant. Therefore, a qualitative regulation of its functions, i.e. enzyme activity and subcellular localization, is required to control cell cycle progression. In the case of CDC25B, the protein accumulates as the cell cycle progresses, reaching a maximum at G2-M phase. Thus, controlling the expression of CDC25B is an effective means of regulating its function. However, at G2 phase, when the CDC25B level is at its peak, an alternate way of keeping it inactive is needed when its activation is inappropriate. Recently, several groups have reported that the binding of 14-3-3, specifically at Ser309 of CDC25B1 or Ser323 of CDC25B2 or CDC25B3, results in the cytoplasmic localization of CDC25B, supporting the theory of its redistribution from the nucleus to the cytoplasm as a critical G2-M checkpoint (Davezac et al., 2000; Forrest and Gabrielli, 2001).

In agreement with these reports, we found that 14-3-3β and 14-3-3ε bound specifically at Ser309 of CDC25B1 and that the binding effectively redistributed CDC25B, decreasing its amount in the nuclei. We consistently detected nuclear localization in about 50% of the CDC25B-transfected cells. Endogenous 14-3-3, detected with a pan-14-3-3 antibody, was recovered as a complex with exogenous CDC25B. The co-expression of 14-3-3β or 14-3-3ε reduced the nuclear localization of exogenous CDC25B by about 20%, but endogenous 14-3-3 was recovered with exogenous CDC25B. More than 95% of the introduced CDC25B was localized in nuclei when the binding of 14-3-3 was abolished by a CDC25B point mutation. Thus, it is reasonable to conclude that the binding of 14-3-3 at Ser309 of CDC25B is essential for the exclusion of CDC25B from the nucleus. We also presented evidence that binding of 14-3-3β to CDC25B slowed down the nuclear import induced by LMB treatment. Since 14-3-3β specifically binds to Ser309, bound 14-3-3 should impair the access of nuclear import cargos, such as importin, to the NLS.

In *Xenopus*, 14-3-3-binding to CDC25C was suggested to mask its NLS, making its nuclear exclusion signal (NES) available for the transfer of CDC25C to the cytoplasm (Kumagai and Dunphy, 1999). The NLS in human CDC25B is located at the same position relative to the 14-3-3-binding site of CDC25C in Xenopus, i.e., about 30 amino acids downstream of Ser309 (Davezac et al., 2000) (S.U., A.K., M.O., M.S., M.H., H.N., T.M., Y.I. and K.Y., unpublished data). Therefore, the binding of 14-3-3β or 14-3-3ε at Ser309 could inactivate the NLS, which in turn would make the N-terminal NES dominant. This idea is further supported by the observation that the preferential binding of 14-3-3σ to Ser216 does not cause cytoplasmic redistribution of CDC25B because Ser216 is too far away to allow 14-3-3σ to mask the NLS. We also conclude from this result that the NES-like sequence present in the C-terminus of all 14-3-3 subtypes does not function as an NES. Thus, our results agree well with the recently presented hypothesis that the binding of 14-3-3 does not add an 'attachable NES' that targets proteins (Rittinger et al., 1999; Brunet et al., 2002). Instead, it might serve other functions, such as providing scaffolding or a cover that hides specific motifs, such as NLS or NES (Muslin and Xing, 2000; Tzivion et al., 2001; Yaffe, 2002).

Ser309 was shown to be phosphorylated by p38 MAP kinase, and the kinase activity was necessary to maintain cell cycle arrest at G2 in response to DNA damage caused by UV light (Bulavin et al., 2001). One of the checkpoint kinases, Chk1, can phosphorylate Ser309 to enhance 14-3-3-binding in vitro (Forrest and Gabrielli, 2001) (S.U., A.K., M.O., M.S., M.H., H.N., T.M., Y.I. and K.Y., unpublished data). Although co-expression of MKK6, Chk1 or Chk2 with CDC25B and 14-3-3β enhanced the binding of 14-3-3β to CDC25B, these effects were not significant (S.U., A.K., M.O., M.S., M.H., H.N., T.M., Y.I. and K.Y., unpublished data). Therefore, Ser309 seems to be constitutively phosphorylated, possibly by p38 or C-TAK1. If phosphorylation of this serine is crucial for the induction and/or maintenance of G2 arrest, the inactivation of the phosphatase responsible for the dephosphorylation might also occur, although enhanced checkpoint kinase activity is usually thought to maintain the phosphorylation state. The significance of the cytoplasmic localization of CDC25B in terms of cell cycle regulation, especially at the G2 checkpoint, is not clear. However, abrogation of the 14-3-3 binding site

abolished G2-arrest and thus caused localization of CDC25B to the nucleus. The overexpression of CDC25B is sufficient to override the G2 DNA damage checkpoint (Miyata et al., 2001), but in this case, Ser309 of the overexpressed CDC25B would be phosphorylated as is the endogenous residue. In addition, the amount of cellular 14-3-3 is obviously in excess of the amount of CDC25B, and thus the equilibrium between 14-3-3-bound CDC25B and unbound CDC25B should be the same in transfected cells and in normal cells. If overexpression enhances the probability of the localization of CDC25B in the nucleus, CDC25B could counteract the inhibitory effects of Wee1 kinase, leading to the activation of CDK1/cyclin B and abrogation of the G2 checkpoint. Phosphorylation of Ser309 should be necessary to inhibit premature mitosis, but it is too early to attribute maintained phosphorylation at the G2 checkpoint to the checkpoint kinases or to p38. So, if Ser309 is constantly phosphorylated, then its phosphorylation level could never be enhanced because of DNA damage (Bulavin et al., 2001). Indeed, no reports indicate a higher than normal phosphorylation level of Ser309 or Ser323 in CDC25B2 or CDC25B3 at the G2 checkpoint, although it is possible to postulate a change from the maintenance kinases to the checkpoint kinases at the checkpoint state to keep the phosphorylation level constant (Bulavin et al., 2002). Thus, the significance of the phosphorylation of Ser309, in combination with the binding of 14-3-3 at the site, must await further conclusions about the G2 checkpoint.

We have reported here the binding of 14-3-3σ at Ser216 of CDC25B, which has not been reported previously. We have also described another site, Ser137, that seems to provide support for the binding of 14-3-3σ. The subtypes 14-3-3β and ε have little preference for either of these sites, although both serine residues partly satisfy the consensus-binding motif of 14-3-3 (RxxS). It is rare to find binding-preference differences among 14-3-3 subtypes and it should be noticed that 14-3-3σ does not prefer Ser309 for binding even though it is in one of the typical 14-3-3 binding motifs. Interestingly, 14-3-3σ also does not bind to CDC25C where Ser216 is located in a typical 14-3-3 binding motif (RSxSMP) (Chan et al., 1999) (S.U., A.K., M.O., M.S., M.H., H.N., T.M., Y.I. and K.Y., unpublished data). Two sites on CDC25B are required for the efficient binding of 14-3-3σ, which means that 14-3-3σ must be a dimer to bind efficiently to the two different sites on CDC25B.

During the preparation of this manuscript an on-line report was published, describing two sites, other than Ser323 of CDC25B2, necessary for 14-3-3 binding (Giles et al., 2003). Those two sites in CDC25B2, Ser151 and Ser230, are exactly the same as Ser137 and Ser216 of CDC25B1 that have been discussed here. We have demonstrated that 14-3-3σ binds to these sites. It is well known that 14-3-3σ is one of the downstream transcriptional targets of p53 (Hermeking et al., 1997). There have been several reports that 14-3-3σ can downregulate CDK activity by binding to it or that 14-3-3σ can move the CDK1/cyclin B complex to the cytoplasm (Bulavin et al., 2002). Here, we suggest that 14-3-3σ downregulates the function of CDC25B and thereby acts as a G2-checkpoint regulator. Our preliminary experiments indicate that the co-expression of CDC25B and Chk1, but not MKK6 (that activates p38), enhances phosphorylation at Ser137 and Ser216 (S.U., A.K., M.O., M.S., M.H., H.N., T.M., Y.I. and K.Y., unpublished data). Further studies are required to determine whether the phosphorylation of both sites leads to the binding of 14-3-3σ and to establish the consequences for CDC25B.

We thank Hiroto Okayama (University of Tokyo) and Minoru Yoshida (RIKEN) for the generous gift of CDC25B1 cDNA and leptomycin B, respectively. This work was supported in part by Grants-in-Aid for Scientific Research (to K.Y. and Y.I.) and for the Second Term of the Comprehensive 10-Year Strategy for Cancer Control (to H.N.) from the Ministry of Health, Labor, and Welfare of Japan.

References

Blasina, A., de Weyer, I. V., Laus, M. C., Luyten, W. H., Parker, A. E. and McGowan, C. H. (1999). A human homologue of the checkpoint kinase Cds1 directly inhibits Cdc25 phosphatase. *Curr. Biol.* **9**, 1-10.

Brunet, A., Kanai, F., Stehn, J., Xu, J., Sarbassova, D., Frangioni, J. V., Dalal, S. N., DeCaprio, J. A., Greenberg, M. E. and Yaffe, M. B. (2002). 14-3-3 transits to the nucleus and participates in dynamic nucleocytoplasmic transport. *J. Cell Biol.* **156**, 817-828.

Bulavin, D. V., Higashimoto, Y., Popoff, I. J., Gaarde, W. A., Basrur, V., Potapova, O., Appella, E. and Fornace, A. J. Jr (2001). Initiation of a G2/M checkpoint after ultraviolet radiation requires p38 kinase. *Nature* **411**, 102-107.

Bulavin, D. V., Amundson, S. A. and Fornace, A. J. (2002). p38 and Chk1 kinases: different conductors for the G(2)/M checkpoint symphony. *Curr. Opin. Genet. Dev.* **12**, 92-97.

Chan, T. A., Hermeking, H., Lengauer, C., Kinzler, K. W. and Vogelstein, B. (1999). 14-3-3Sigma is required to prevent mitotic catastrophe after DNA damage. *Nature* **401**, 616-620.

Chan, T. A., Hwang, P. M., Hermeking, H., Kinzler, K. W. and Vogelstein, B. (2000). Cooperative effects of genes controlling the G(2)/M checkpoint. *Genes Dev.* **14**, 1584-1588.

Chow, J. P., Siu, W. Y., Fung, T. K., Chan, W. M., Lau, A., Arooz, T., Ng, C. P., Yamashita, K. and Poon, R. Y. (2003). DNA damage during the spindle-assembly checkpoint degrades CDC25A, inhibits cyclin-CDC2 complexes, and reverses cells to interphase. *Mol. Biol. Cell* **14**, 3989-4002.

Conklin, D. S., Galaktionov, K. and Beach, D. (1995). 14-3-3 proteins associate with cdc25 phosphatases. *Proc. Natl. Acad. Sci. USA* **92**, 7892-7896.

Davezac, N., Baldin, V., Gabrielli, B., Forrest, A., Theis-Febvre, N., Yashida, M. and Ducommun, B. (2000). Regulation of CDC25B phosphatases subcellular localization. *Oncogene* **19**, 2179-2185.

Ford, J. C., al-Khodairy, F., Fotou, E., Sheldrick, K. S., Griffiths, D. J. and Carr, A. M. (1994). 14-3-3 protein homologs required for the DNA damage checkpoint in fission yeast. *Science* **265**, 533-535.

Forrest, A. and Gabrielli, B. (2001). Cdc25B activity is regulated by 14-3-3. *Oncogene* **20**, 4393-4401.

Furnari, B., Blasina, A., Boddy, M. N., McGowan, C. H. and Russell, P. (1999). Cdc25 inhibited in vivo and in vitro by checkpoint kinases Cds1 and Chk1. *Mol. Biol. Cell.* **10**, 833-845.

Galaktionov, K. and Beach, D. (1991). Specific activation of cdc25 tyrosine phosphatases by B-type cyclins: evidence for multiple roles of mitotic cyclins. *Cell* **67**, 1181-1194.

Galaktionov, K., Lee, A. K., Eckstein, J., Draetta, G., Meckler, J., Loda, M. and Beach, D. (1995). CDC25 phosphatases as potential human oncogenes. *Science* **269**, 1575-1577.

Giles, N., Forrest, A. and Gabrielli, B. (2003). 14-3-3 acts as an intramolecular bridge to regulate cdc25B localization and activity. *J. Biol. Chem.* **278**, 28580-28587.

Graves, P. R., Lovly, C. M., Uy, G. L. and Piwnica-Worms, H. (2001). Localization of human Cdc25C is regulated both by nuclear export and 14-3-3 protein binding. *Oncogene* **20**, 1839-1851.

Hermeking, H., Lengauer, C., Polyak, K., He, T. C., Zhang, L., Thiagalingam, S., Kinzler, K. W. and Vogelstein, B. (1997). 14-3-3 sigma is a p53-regulated inhibitor of G2/M progression. *Mol. Cell* **1**, 3-11.

Honda, R., Ohba, Y. and Yasuda, H. (1997). 14-3-3 zeta protein binds to the carboxyl half of mouse wee1 kinase. *Biochem. Biophys. Res. Commun.* **230**, 262-265.

Hutchins, J. R., Hughes, M. and Clarke, P. R. (2000). Substrate specificity determinants of the checkpoint protein kinase Chk1. *FEBS Lett.* **466**, 91-95.

Karlsson, C., Katich, S., Hagting, A., Hoffmann, I. and Pines, J. (1999). Cdc25B and Cdc25C differ markedly in their properties as initiators of mitosis. *J. Cell. Biol.* **146**, 573-584.

Kudo, N., Wolff, B., Sekimoto, T., Schreiner, E. P., Yoneda, Y., Yanagida, M., Horinouchi, S. and Yoshida, M. (1998). Leptomycin B inhibition of signal-mediated nuclear export by direct binding to CRM1. *Exp. Cell Res.* **242**, 540-547.

Kumagai, A. and Dunphy, W. G. (1999). Binding of 14-3-3 proteins and nuclear export control the intracellular localization of the mitotic inducer Cdc25. *Genes Dev.* **13**, 1067-1072.

Kumagai, A., Yakowec, P. S. and Dunphy, W. G. (1998). 14-3-3 proteins act as negative regulators of the mitotic inducer Cdc25 in Xenopus egg extracts. *Mol. Biol. Cell* **9**, 345-354.

Lammer, C., Wagerer, S., Saffrich, R., Mertens, D., Ansorge, W. and Hoffmann, I. (1998). The cdc25B phosphatase is essential for the G2/M phase transition in human cells. *J. Cell Sci.* **111**, 2445-2453.

Lee, J., Kumagai, A. and Dunphy, W. G. (2001). Positive regulation of Wee1 by Chk1 and 14-3-3 proteins. *Mol. Biol. Cell* **12**, 551-563.

Ma, Z. Q., Chua, S. S., DeMayo, F. J. and Tsai, S. Y. (1999). Induction of mammary gland hyperplasia in transgenic mice over-expressing human Cdc25B. *Oncogene* **18**, 4564-4576.

Mailand, N., Podtelejnikov, A. V., Groth, A., Mann, M., Bartek, J. and Lukas, J. (2002). Regulation of G2/M events by Cdc25A through phosphorylation-dependent modulation of its stability. *EMBO J.* **21**, 5911-5920.

Matsuoka, S., Huang, M. and Elledge, S. J. (1998). Linkage of ATM to cell cycle regulation by the Chk2 protein kinase. *Science* **282**, 1893-1897.

Mils, V., Baldin, V., Goubin, F., Pinta, I., Papin, C., Waye, M., Eychene, A. and Ducommun, B. (2000). Specific interaction between 14-3-3 isoforms and the human CDC25B phosphatase. *Oncogene* **19**, 1257-1265.

Miyata, H., Doki, Y., Yamamoto, H., Kishi, K., Takemoto, H., Fujiwara, Y., Yasuda, T., Yano, M., Inoue, M., Shiozaki, H. et al. (2001). Overexpression of CDC25B overrides radiation-induced G2-M arrest and results in increased apoptosis in esophageal cancer cells. *Cancer Res.* **61**, 3188-3193.

Morgan, D. O. (1997). Cyclin-dependent kinases: engines, clocks, and microprocessors. *Annu. Rev. Cell Dev. Biol.* **13**, 261-291.

Muslin, A. J. and Xing, H. (2000). 14-3-3 proteins: regulation of subcellular localization by molecular interference. *Cell. Signal.* **12**, 703-709.

Muslin, A. J., Tanner, J. W., Allen, P. M. and Shaw, A. S. (1996). Interaction of 14-3-3 with signaling proteins is mediated by the recognition of phosphoserine. *Cell* **84**, 889-897.

Nagata, A., Igarashi, M., Jinno, S., Suto, K. and Okayama, H. (1991). An additional homolog of the fission yeast cdc25+ gene occurs in humans and is highly expressed in some cancer cells. *New Biol.* **3**, 959-968.

Nilsson, I. and Hoffmann, I. (2000). Cell cycle regulation by the Cdc25 phosphatase family. *Prog. Cell Cycle Res.* **4**, 107-114.

Nishi, K., Yoshida, M., Fujiwara, D., Nishikawa, M., Horinouchi, S. and Beppu, T. (1994). Leptomycin B targets a regulatory cascade of crm1, a fission yeast nuclear protein, involved in control of higher order chromosome structure and gene expression. *J. Biol. Chem.* **269**, 6320-6324.

O'Neill, T., Giarratani, L., Chen, P., Iyer, L., Lee, C. H., Bobiak, M., Kanai, F., Zhou, B. B., Chung, J. H. and Rathbun, G. A. (2002). Determination of substrate motifs for human Chk1 and hCds1/Chk2 by the oriented peptide library approach. *J. Biol. Chem.* **277**, 16102-16115.

Peng, C. Y., Graves, P. R., Thoma, R. S., Wu, Z., Shaw, A. S. and Piwnica-Worms, H. (1997). Mitotic and G2 checkpoint control: regulation of 14-3-3 protein binding by phosphorylation of Cdc25C on serine-216. *Science* **277**, 1501-1505.

Peng, C. Y., Graves, P. R., Ogg, S., Thoma, R. S., Byrnes, M. J. 3rd, Wu, Z., Stephenson, M. T. and Piwnica-Worms, H. (1998). C-TAK1 protein kinase phosphorylates human Cdc25C on serine 216 and promotes 14-3-3 protein binding. *Cell Growth Differ.* **9**, 197-208.

Rittinger, K., Budman, J., Xu, J., Volinia, S., Cantley, L. C., Smerdon, S. J., Gamblin, S. J. and Yaffe, M. B. (1999). Structural analysis of 14-3-3 phosphopeptide complexes identifies a dual role for the nuclear export signal of 14-3-3 in ligand binding. *Mol. Cell* **4**, 153-166.

Rothblum-Oviatt, C. J., Ryan, C. E. and Piwnica-Worms, H. (2001). 14-3-3 binding regulates catalytic activity of human Wee1 kinase. *Cell Growth Differ.* **12**, 581-589.

Sanchez, Y., Wong, C., Thoma, R. S., Richman, R., Wu, Z., Piwnica-Worms, H. and Elledge, S. J. (1997). Conservation of the Chk1 checkpoint pathway in mammals: linkage of DNA damage to Cdk regulation through Cdc25. *Science* **277**, 1497-1501.

Sebastian, B., Kakizuka, A. and Hunter, T. (1993). Cdc25M2 activation of cyclin-dependent kinases by dephosphorylation of threonine-14 and tyrosine-15. *Proc. Natl. Acad. Sci. USA* **90**, 3521-3524.

Tzivion, G., Shen, Y. H. and Zhu, J. (2001). 14-3-3 proteins; bringing new definitions to scaffolding. *Oncogene* **20**, 6331-6338.

Wang, Y., Jacobs, C., Hook, K. E., Duan, H., Booher, R. N. and Sun, Y. (2000). Binding of 14-3-3beta to the carboxyl terminus of Wee1 increases Wee1 stability, kinase activity, and G2-M cell population. *Cell Growth Differ.* **11**, 211-219.

Wang, X., Arooz, T., Siu, W. Y., Chiu, C. H., Lau, A., Yamashita, K. and Poon, R. Y. (2001). MDM2 and MDMX can interact differently with ARF and members of the p53 family. *FEBS Lett.* **490**, 202-208.

Yaffe, M. B. (2002). How do 14-3-3 proteins work? Gatekeeper phosphorylation and the molecular anvil hypothesis. *FEBS Lett.* **513**, 53-57.

Yaffe, M. B., Rittinger, K., Volinia, S., Caron, P. R., Aitken, A., Leffers, H., Gamblin, S. J., Smerdon, S. J. and Cantley, L. C. (1997). The structural basis for 14-3-3: phosphopeptide binding specificity. *Cell* **91**, 961-971.

Yang, J., Winkler, K., Yoshida, M. and Kornbluth, S. (1999). Maintenance of G2 arrest in the Xenopus oocyte: a role for 14-3-3-mediated inhibition of Cdc25 nuclear import. *EMBO J.* **18**, 2174-2183.

Yao, Y., Slosberg, E. D., Wang, L., Hibshoosh, H., Zhang, Y. J., Xing, W. Q., Santella, R. M. and Weinstein, I. B. (1999). Increased susceptibility to carcinogen-induced mammary tumors in MMTV-Cdc25B transgenic mice. *Oncogene* **18**, 5159-5166.

Girolline, an Antitumor Compound Isolated from a Sponge, Induces G2/M Cell Cycle Arrest and Accumulation of Polyubiquitinated p53

Sachiko TSUKAMOTO,*[a] Katsumi YAMASHITA,[a] Kazuhiro TANE,[a] Ryoichi KIZU,[a] Tomihisa OIITA,[a] Shigeki MATSUNAGA,[b] Nobuhiro FUSETANI,[b] Hiroyuki KAWAHARA,[c] and Hideyoshi YOKOSAWA[c]

[a] *Faculty of Pharmaceutical Sciences, Kanazawa University; Kanazawa 920–0934, Japan:* [b] *Laboratory of Aquatic Natural Products Chemistry, Graduate School of Agricultural and Life Sciences, The University of Tokyo; Bunkyo-ku, Tokyo 113–8657, Japan: and* [c] *Department of Biochemistry, Graduate School of Pharmaceutical Sciences, Hokkaido University; Sapporo 060–0812, Japan.* Received January 5, 2004; accepted February 10, 2004; published online February 12, 2004

Girolline, an antitumor compound isolated from a sponge, has been reported to inhibit the termination step of protein synthesis *in vivo*. In this study, we found that girolline induced G2/M cell cycle arrest in several tumor cell lines. Immunochemical analysis revealed that polyubiquitinated p53 was accumulated in girolline-treated cells, while other polyubiquitinated cellular proteins were not accumulated, indicating that the effect of girolline is specific for p53. On the other hand, girolline did not inhibit proteasome activity *in vitro*, and accumulation of polyubiquitinated p53 was scarcely detected in the presence of leptomycin B, an inhibitor of nuclear export. Based on the above findings, we propose that girolline affects the step of recruitment of polyubiquitinated p53 to the proteasome.

Key words girolline; cell cycle; ubiquitin; p53; proteasome

The ubiquitin-dependent proteolytic pathway plays a major role in selective protein degradation.[1—4] Ubiquitin attaches to a target protein prior to degradation. Ubiquitination of proteins requires the sequential actions of the ubiquitin-activating enzyme (E1), ubiquitin-conjugating enzymes (E2s), and ubiquitin-protein ligases (E3s). The polyubiquitin chains thus formed are recognized by the 26S proteasome, an intracellular high-molecular-mass protease subunit complex, and the protein portion is degraded by the proteolytic active sites in a cavity in the 26S proteasome.[1,2] The stability of short-lived proteins, including p53, is regulated through the ubiquitin-dependent proteolytic pathway. The tumor suppressor protein p53 controls cell growth and development of genetic abnormalities through G1 arrest or apoptosis in response to DNA damage.[5,6]

Girolline, a 2-aminoimidazole derivative, was originally isolated as an antitumor compound from the marine sponge *Pseudaxinyssa cantharella* collected in New Caledonia.[7] This compound exhibits significant cytotoxicity *in vitro* against several tumor cell lines and *in vivo* against murine grafted tumors, including P388 and L1210 leukemias, and solid tumors.[8] Although its structure suggests it has alkylating activity toward nucleic acids, biochemical study revealed that girolline is not an alkylating agent but is a protein synthesis inhibitor.[8] Further study suggested that girolline inhibits the termination step of protein synthesis.[9] Since toxicological study using dogs and mice suggested that girolline has little toxic effect, a phase I clinical study has been conducted. However, it was found that girolline had severe side effects in patients but no apparent antitumor activity.[10]

Recently, we isolated girolline from another species of the marine sponge *Axinella brevistyla* collected in western Japan. We found that cells treated with girolline exhibited G2/M cell cycle arrest. An immunochemical study showed that girolline induced the accumulation of polyubiquitinated p53 but not that of other polyubiquitinated cellular proteins. On the other hand, girolline did not inhibit activity of the proteasome *in vitro*. Thus, the results suggest that girolline affects the step of recruitment of polyubiquitinated p53 to the proteasome.

MATERIALS AND METHODS

Materials Girolline was isolated from the marine sponge *Axinella brevistyla* as previously reported.[11] Leptomycin B was a gift from Dr. M. Yoshida of RIKEN, Wako, Japan.

Cell Culture FL, HeLa and A549 cells were cultured in Dulbecco's modified Eagle's medium supplemented with 10% fetal calf serum, penicillin (100 units/ml), and streptomycin (100 μg/ml) under a humidified atmosphere of 5% CO_2 at 37 °C.

Flow Cytometric Analysis Cells were harvested by trypsin digestion, washed with cold phosphate-buffered saline (PBS), and fixed with ice-cold 70% ethanol. The fixed cells were collected by brief centrifugation and treated with PBS containing 500 μg/ml RNase A (Sigma) at 37 °C for 20 min and then with 10 μg/ml propidium iodide (Wako Pure Chemicals) at room temperature for 15 min. Samples were then subjected to flow cytometric analysis by using a FACScalibur (Becton-Dickinson Immunocytometer Systems).

Preparation of Cell Extracts and Immunoprecipitation The cells were disrupted with ice-cold buffer A consisting of 20 mM Tris–HCl, pH 7.5, 5 mM EDTA, 150 mM NaCl, 1% Nonidet P-40, 5 mM *N*-ethylmaleimide, 10 μM MG132 (Peptide Institute), and a proteasome inhibitor cocktail (Roche). After removing cell debris by centrifugation, the resulting supernatant was used as the cell extract. To immuoprecipitate p53, anti-p53 antibody-immobilized agarose beads (Santa Cruz) were added to the cell extract, and the mixture was stirred at 4 °C for 2 h and centrifuged at 15000 rpm for 1 min. After the precipitated beads had been extensively washed with buffer A, the materials bound to the beads were subjected to SDS-PAGE and then to Western blotting as described below.

Gel Electrophoresis and Western Blotting SDS-PAGE was carried out in a slab gel containing 12% polyacrylamide. After SDS-PAGE and blotting to the membranes, blocking

* To whom correspondence should be addressed. e-mail: sachiko@p.kanazawa-u.ac.jp

with 5% skim milk in PBS containing 0.1% Tween 20 and immunoblotting were carried out. For immunochemical detection of p53 and ubiquitin, a mouse monoclonal antibody against human p53 (Santa Cruz) and a rabbit polyclonal antibody against bovine ubiquitin (DAKO), respectively, were used as primary antibodies and peroxidase-conjugated anti-mouse IgG or anti-rabbit IgG (Amersham) was used as a secondary antibody. For detection of polyubiquitin chains, FK1 antibody, which specifically recognizes polyubiquitin chains,[12] and biotin-conjugated anti-mouse IgM (Amersham) were used as the first and second antibodies, respectively. Detection was performed using an enhanced chemiluminescence system (Amersham), and bands were visualized with X-ray film.

Preparation of Proteasome-Enriched Fraction FL cells were centrifuged at 1000 rpm for 5 min, and the resultant packed cells were suspended in ice-cold buffer B consisting of 20 mM HEPES, pH 7.5, 5 mM KCl, 1.5 mM $MgCl_2$, 1 mM dithiothreitol, 2 mM ATP, and 10% glycerol and were then disrupted by a Teflon homogenizer at 4 °C for 5 min. The cell lysate was immediately centrifuged at 10000 rpm for 5 min, and the resultant supernatant was further centrifuged at 100000×*g* for 5 h. The precipitates thus obtained were suspended in buffer B and used as a proteasome-enriched preparation.

Assay for Proteasome Activity The fluorogenic substrate Suc-Leu-Leu-Val-Tyr-MCA (Peptide Institute) was used as a substrate for chymotrypsin-like activity of the proteasome. The ATP-activated activity of the proteasome was measured at 37 °C for 30 min using the above proteasome-enriched preparation in a reaction mixture (1 ml) that contained 50 mM Tris–HCl, pH 7.8, 1 mM dithiothreitol, 10 mM $MgCl_2$, 2 mM ATP, 0.05 mM substrate, and an enzyme solution (5 μl), and the reaction was stopped by adding 1 ml of 10% SDS. The fluorescence intensity derived from 7-amino-4-methylcoumarin (excitation, 380 nm; emission, 460 nm) was measured using a Shimadzu spectrofluorophotometer RF-5000.

RESULTS AND DISCUSSION

Girolline Induces G2/M Cell Cycle Arrest Girolline has been reported to inhibit protein synthesis.[8,9] Since we also isolated girolline from another species of the marine sponge, we first carried out an experiment to determine whether girolline affects the cell cycles of several tumor cell lines. FL, HeLa, and A549 cells were cultured in the presence of 50 μM girolline for 24 h, washed with PBS, fixed, and stained with propidium iodide. The stained cells were then subjected to flow cytometric analysis to examine the cell cycle profile. As shown in Fig. 1, girolline was found to induce G2/M cell cycle arrest in FL cells. Girolline-induced G2/M arrest was also observed in HeLa and A549 cells, though to a lesser extent (data not shown).

Polyubiquitinated p53 Accumulates in Girolline-Treated Cells The tumor suppressor p53 has been reported to be involved in G2 cell cycle arrest as well as in G1 arrest.[5,6,13] Since we found that girolline induced G2/M cell cycle arrest, we next carried out an experiment to determine the relationship between girolline and p53. FL cells were cultured in the presence of 50 μM girolline for 24 h, and the cell extract was prepared and subjected to SDS-PAGE followed by Western blotting with anti-p53 antibody. Several bands with higher molecular masses than that of the original p53 were detected (data not shown). To characterize the high-molecular-mass bands of p53, the cell extract was subjected to immunoprecipitation using anti-p53 antibody-immobilized agarose, and the immunoprecipitates thus formed were then subjected to Western blotting with anti-p53 and anti-ubiquitin antibodies (Fig. 2). It was found that, among the bands recognized by anti-p53 antibody, two bands with 70 kDa and 58 kDa also immunoreacted with anti-ubiquitin antibody, indicating that the immunoreactive bands are derived from polyubiquitinated p53. In addition, it should be noted that the bands recognized by both antibodies became stronger as the concentration of girolline used was increased. These results indicate that girolline induces accumulation of polyubiquitinated p53 in a concentration-dependent manner. The absence of two anti-p53 immunoreactive bands with 70 and 58 kDa in control may be partly due to the difference in sensitivity of antibodies used.

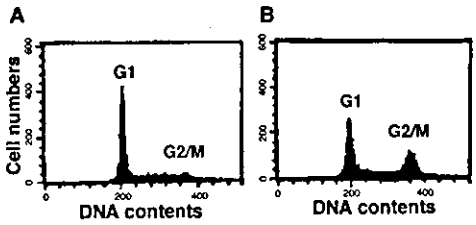

Fig. 1. Girolline Induces G2/M Cell Cycle Arrest

FL cells were cultured in the absence (A) or presence (B) of 50 μM girolline for 24 h, harvested, and subjected to flow cytometric analysis. The positions of G1 and G2/M are labeled.

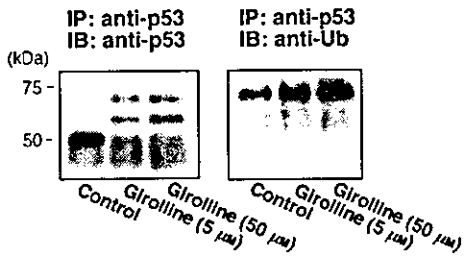

Fig. 2. Girolline Induces Accumulation of Polyubiquitinated p53

FL cells were cultured in the presence of girolline for 24 h, and the cell extract was prepared and subjected to immunoprecipitation (IP) using anti-p53 antibody-immobilized agarose. The immunoprecipitates thus formed were then subjected to Western blotting with anti-p53 (*left panel*) and anti-ubiquitin (anti-Ub) (*right panel*) antibodies. IB, immunoblotting.

Girolline Is Unable to Inhibit the Activity of the Proteasome and Nuclear Export of p53 To determine whether the accumulation of polyubiquitinated p53, induced by girolline treatment, was due to its inhibition of the activity of the proteasome, we assayed chymotrypsin-like activity of the proteasome toward Suc-Leu-Leu-Val-Tyr-MCA in the presence of girolline. It was found that girolline did not inhibit the proteasome activity even at the concentration of 200 μM, while MG132 at 10 μM completely inhibited the proteasome activity. In contrast, MG132 induced accumulation of polyubiquitinated p53 as girolline did (see Fig. 3).

It has been reported that some proteins such as p27, a cyclin-dependent kinase inhibitor, are polyubiquitinated/degraded inside the nucleus, or, alternatively, are exported to